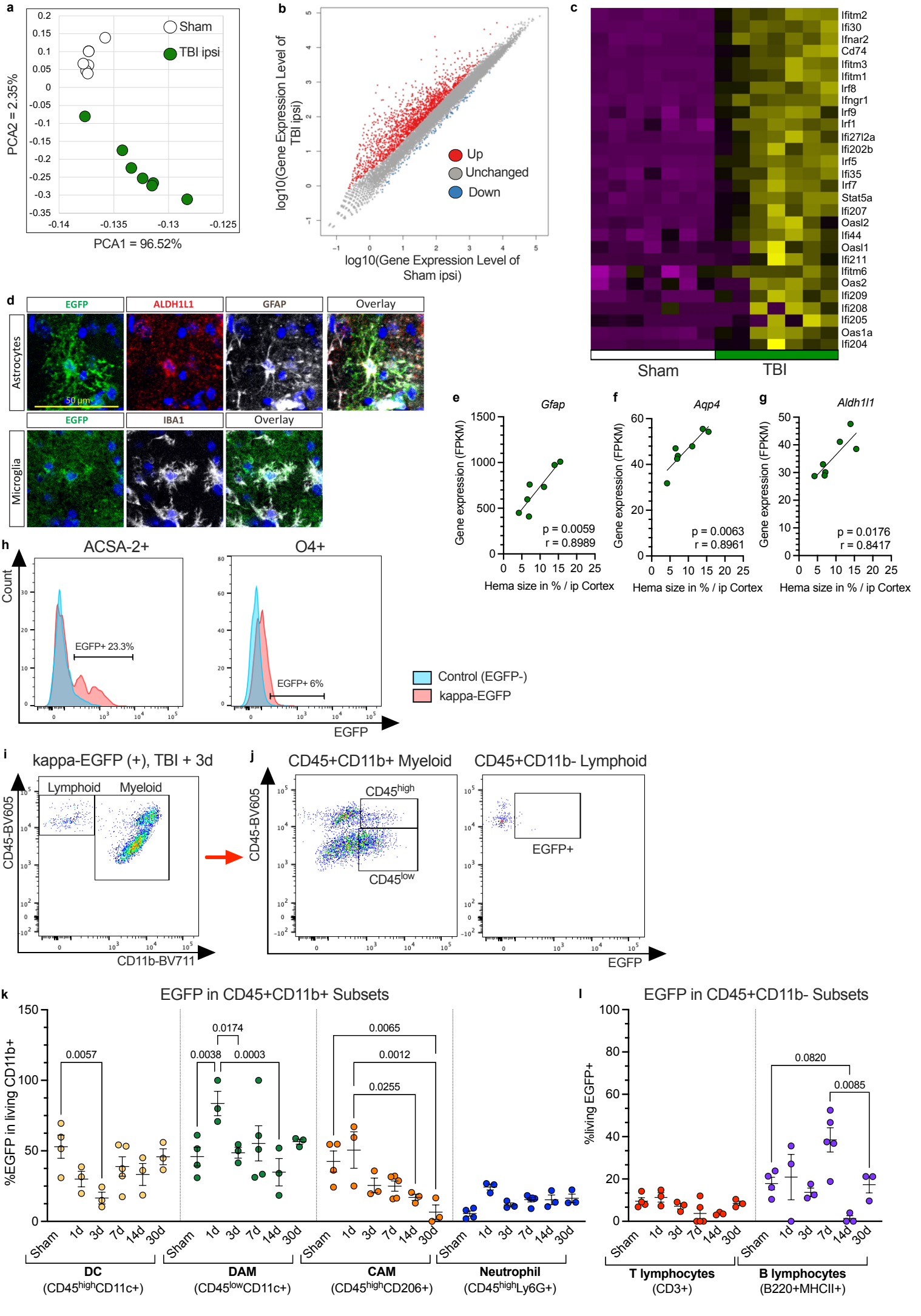
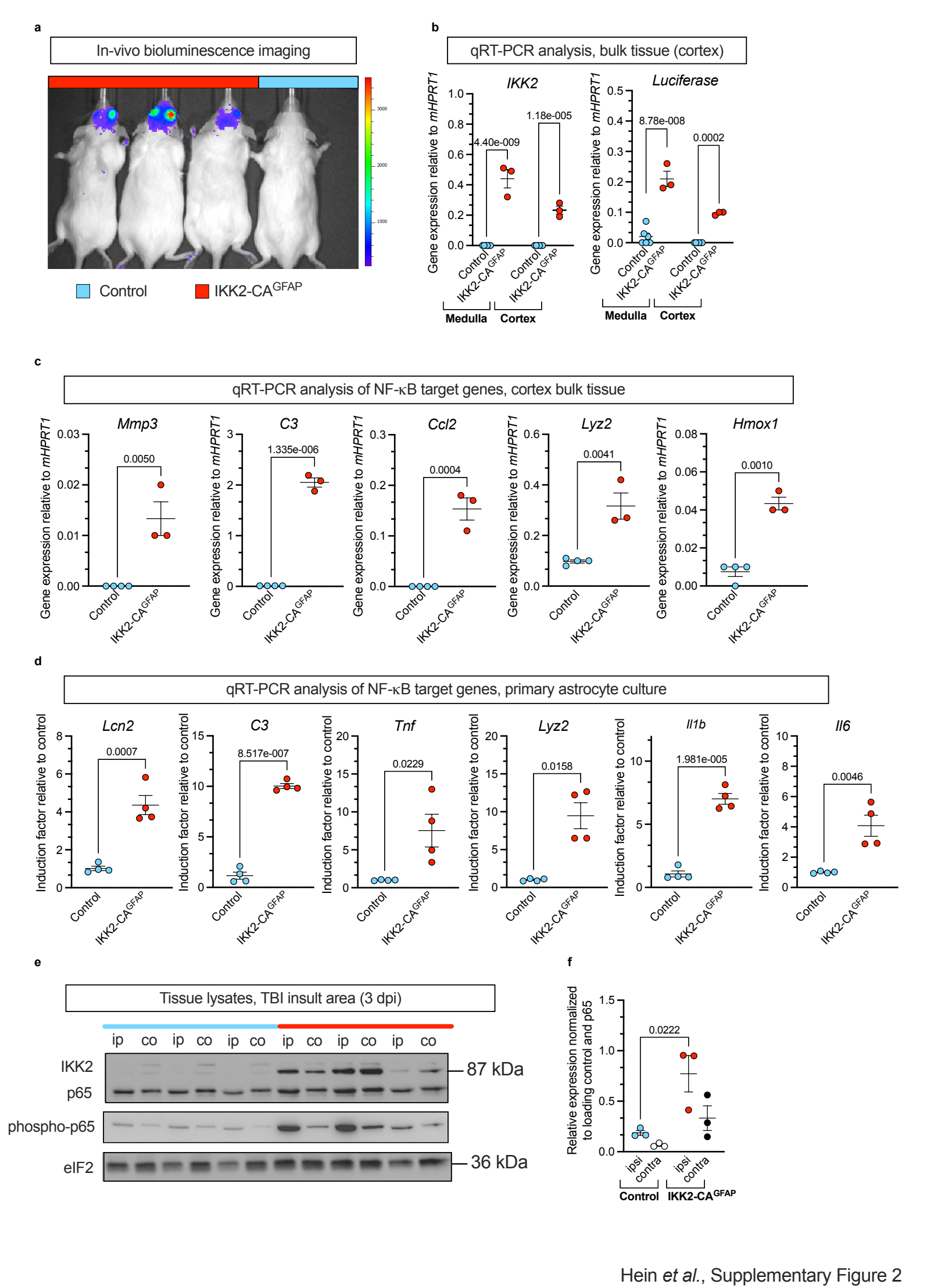


Hein *et al.*, Supplementary Figure 1

Supplementary Figure 1: TBI activates NF-κB expression in a cell type-specific and time-dependent manner

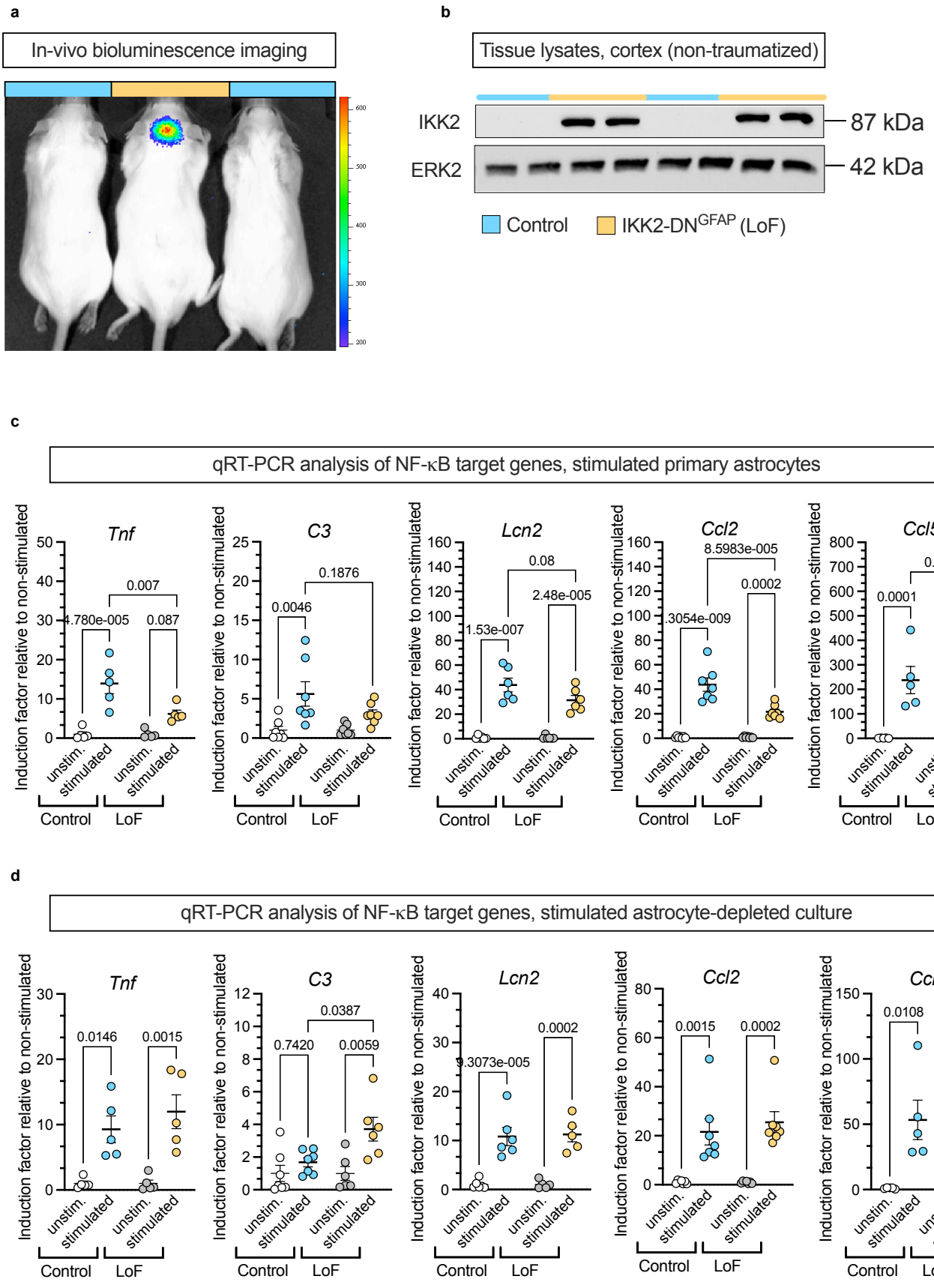
(a) PCA analysis of RNA samples derived from traumatized bulk tissue (ipsilateral insult area) from TBI and sham treated wildtype mice 3 days after CHI/TBI (3 dpi; n = 7 per group). PCA1 is plotted on the x-axis, while the y-axis shows PCA2. (b) Scatter plot of transcriptomic profile after TBI is shown. Gene expression levels (presented as $\log_{10}$) of wildtype animals with TBI are plotted against sham-treated group. Red – upregulated genes ($\log_2$FoldChange ≥ 1, padj ≤ 0.05); blue – downregulated genes ($\log_2$FoldChange ≤ -1, padj ≤.0,05). (c) Heat map depicting the upregulation of interferon-associated genes in the insult area of TBI (green) and sham-treated animals (white). (d) Representative image of NF-κB positive astrocytes identified by EGFP, ALDH1L1 and GFAP and microglia by EGFP and IBA1 costaining as indicated. (e, f, g) Correlation of gene expression (Fragments Per Kilobase per Million mapped fragments, FPKM) with hematoma size in the insult region (hematoma size is presented in % of the total ipsilateral cortex). The strength of expression of the astrocyte identity genes (e) *Gfap,* (f) *Aqp4* and (g) *Aldh1l1* show a significant correlation and positive dependence on hematoma size by simple linear regression. (h) Representative histograms of EGFP-positive signals in ACSA-2+ and O4+ population with the corresponding negative control at day 3 post TBI. (i, j) Gating strategy for (i) identification and (j) EGFP expression in lymphoid and myeloid cells at day 3 post TBI. (k, l) Quantification of NF-κB/EGFP activity in various (k) myeloid (dendritic cells – yellow, DAM – green, CAM – orange, neutrophils – dark blue) and (l) lymphoid subsets (T lymphocytes – red, B lymphocytes – purple) over time after TBI as indicated. Exact significances indicated in graphs. Source data are provided as a Source Data file.



Hein *et al.*, Supplementary Figure 2

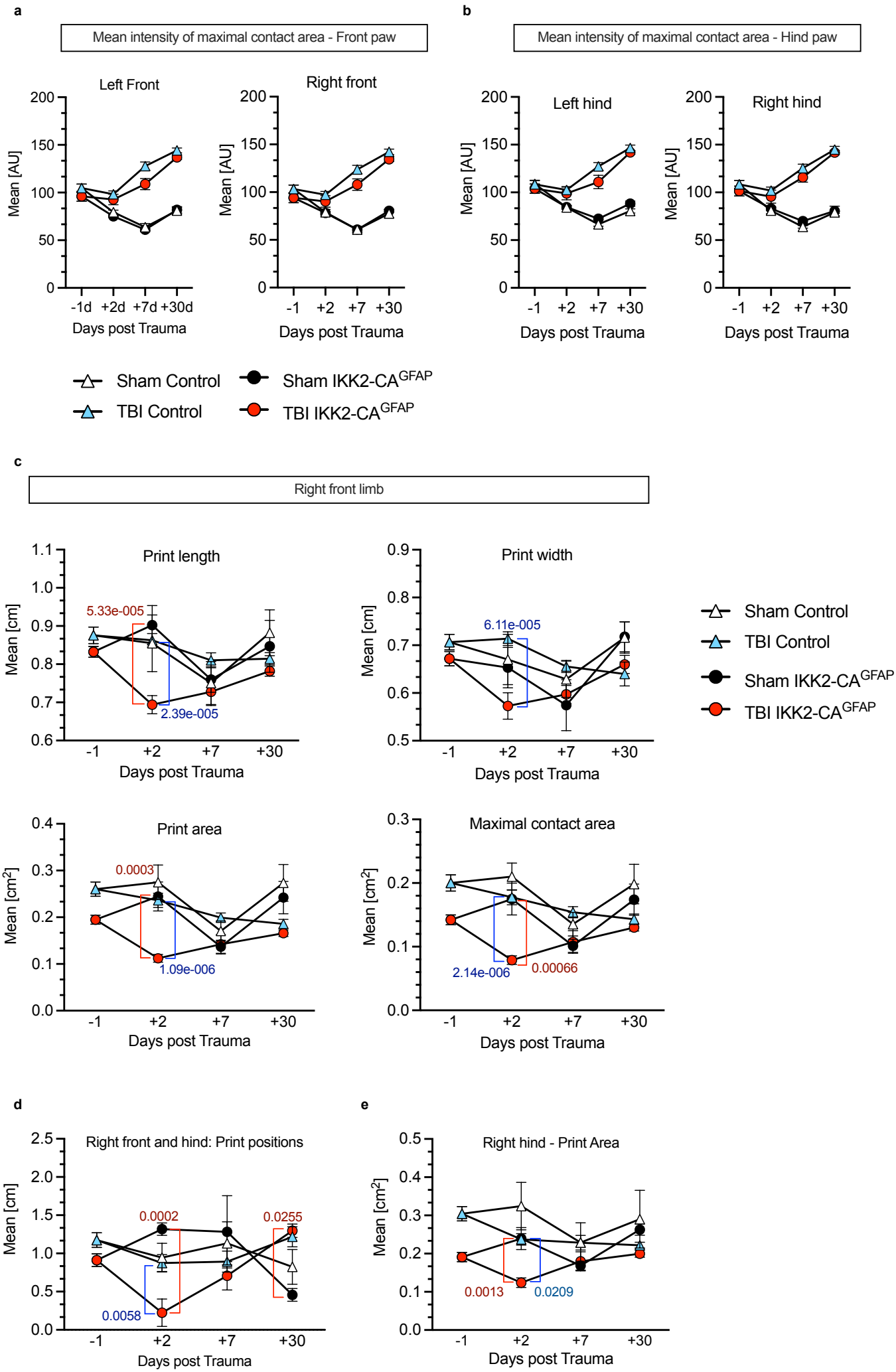
Supplementary Figure 2: Functional validation of the IKK2-CA^{GFAP} mouse model.

(a) *In-vivo* (IVIS) imaging of IKK2-CA^{GFAP} animals and control littermates. Bioluminescent signals (radiance) are restricted to animals with IKK2-CA transgene expression and co-expressed luciferase reporter gene (b) Expression of *hIKK2-CA transgene* and the luciferase reporter gene in the cortex of non-traumatized control (blue) and IKK2-CA^{GFAP} (red) mice by quantitative RT-PCR. (c) Expression levels of various NF-κB target genes in bulk tissue derived from the cerebral cortex of untreated animals as indicated. Elevated NF-κB target gene expression in IKK2-CA^{GFAP} cortex confirms transgene functionality (d) RT-qPCR analysis of different NF-κB target genes as depicted do confirm elevated IKK/NF-κB signaling in primary control and IKK2-CA^{GFAP} astrocyte cultures. Statistical comparison by unpaired, two-tailed t-test. Exact significances indicated in graphs. (e) Immunoblot analysis of IKK2-CA transgene, p65 (NF-κB subunit) and phspho-p65 expression together with eIF2 loading control using tissue lysates of the ipsi- (ip) and contralateral (co) TBI insult area at day 3 post TBI (see also Figure 8b). (f) Corresponding quantification of phosphorylation of the p65 subunit indicates activated NF-κB in GoF mice which depends on IKK2-CA transgene expression strength. Bars indicate Mean±SEM. Statistical comparison by ordinary one-way ANOVA with Tukey's multiple comparisons test. Exact significances indicated in graphs. Source data are provided as a Source Data file.


a
In-vivo bioluminescence imaging
b
Tissue lysates, cortex (non-traumatized)
IKK2
ERK2
87 kDa
42 kDa
Control
IKK2-DNGFAP (LoF)
c
qRT-PCR analysis of NF-κB target genes, stimulated primary astrocytes
Tnf
C3
Lcn2
Ccl2
Ccl5
Induction factor relative to non-stimulated
unstim.
stimulated
Control
LoF
4.780e-005
0.087
0.007
0.0046
0.1876
1.53e-007
2.48e-005
0.08
.3054e-009
0.0002
8.5983e-005
0.0001
0.0006
d
qRT-PCR analysis of NF-κB target genes, stimulated astrocyte-depleted culture
0.0146
0.0015
0.7420
0.0059
0.0387
9.3073e-005
0.0002
0.0015
0.0002
0.0108
0.0055

Supplementary Figure 3: Functional validation of the IKK2-DN^{GFAP} mouse model.

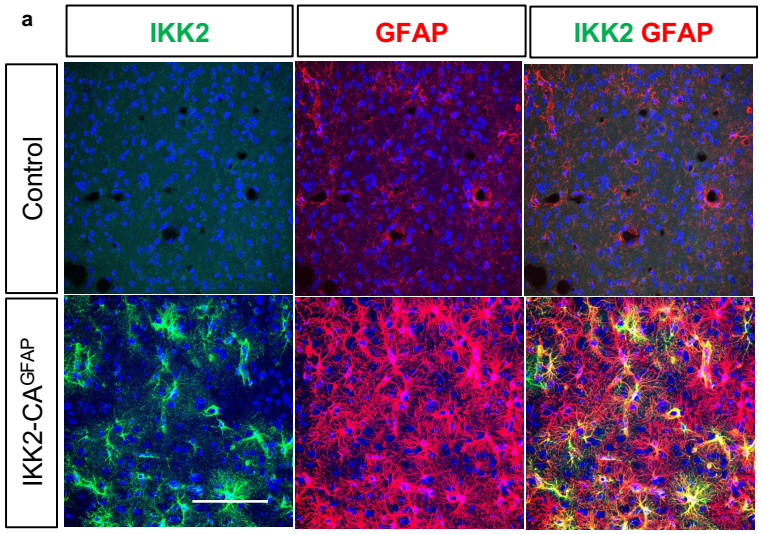
(a) *In-vivo* (IVIS) imaging of IKK2-DN^{GFAP} (yellow) animals and control (blue) littermates. Bioluminescent signal (radiance) is restricted to the animal with IKK2-DN transgene expression and co-expressed luciferase reporter gene (b) Immunoblot analysis of IKK2-DN transgene expression together with ERK2 loading control using tissue lysates derived from the cerebral cortex of untreated IKK2-DN^{GFAP} animals and control littermate as indicated. (c) qRT-qPCR analysis of different NF-κB target genes as depicted with (control – blue, LoF – yellow) or without (control – white, IKK2-LoF – gray) LPS/TNF/Poly I:C stimulation revealed strong repression but not a complete blockade of NF-κB target gene expression in primary IKK2-DN^{GFAP} astrocyte cultures as indicated. (d) qRT-qPCR analysis using astrocyte depleted primary brain cells from IKK2-DN^{GFAP} mice, which did not show inhibition of stimulus-induced NF-κB target gene expression thus confirming astrocyte specificity. Statistical comparison by one-way ANOVA with Tukey's multiple comparisons test. Exact significances indicated in graphs. Source data are provided as a Source Data file.

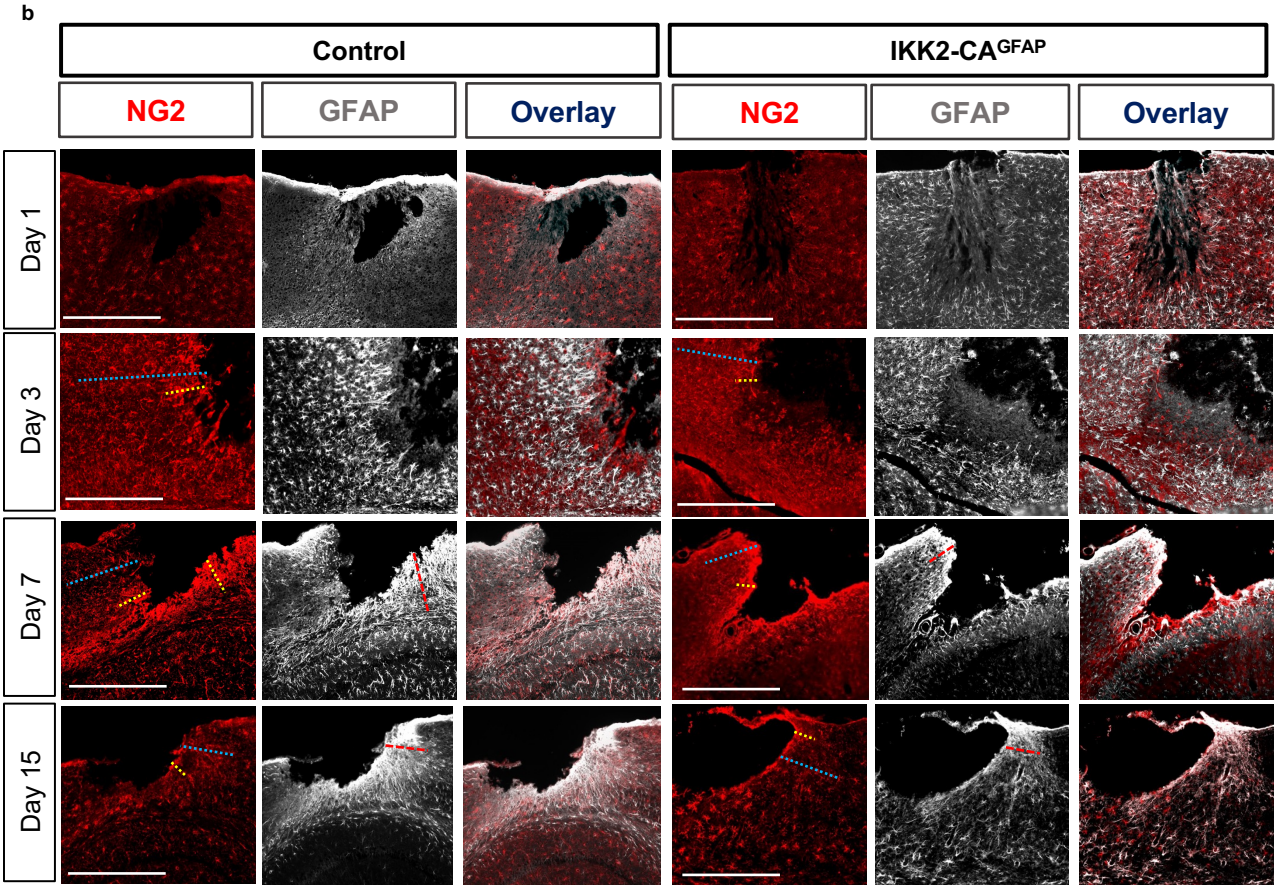


Hein *et al.*, Supplementary Figure 4

Supplementary Figure 4: CatWalk™ XT gait analysis revealed transient behavioral deficits in IKK2-CA^{GFAP} animals.

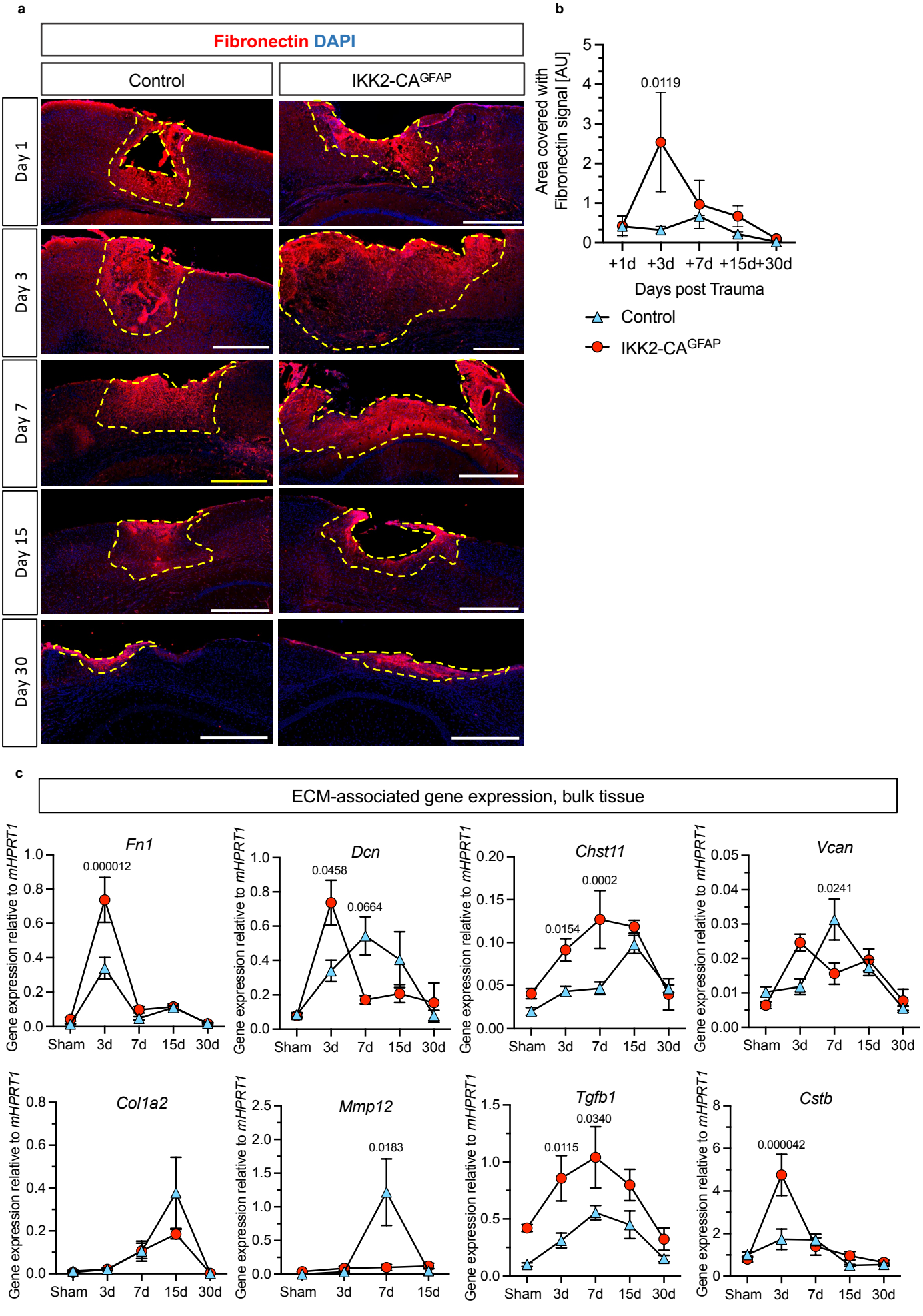
Mean intensity of maximal contact area (measured in arbitrary units, AU) of the left and right (a) front and (b) hind paws prior to and after sham-treatment or TBI as indicated. (c) Gait parameters of the right front paw before and after sham-treatment or TBI. Mean values of print length [cm], width [cm] and area [cm^2], as well as the maximal contact area [cm^2] are presented showing significant differences in the GoF model at day 2 post TBI. Measurements of (d) print positions (in cm) of the right front and hind paw and (e) print area (in cm^2) of the right hind paw. Data were obtained using the CatWalk™ XT gait analysis system before (-1) and at day 2, 7 and 30 post treatment. Data points of sham and TBI animals are pooled for control and IKK2-CA^{GFAP} genotypes at day 1. Blue lines indicate comparison between TBI IKK2-CA^{GFAP} and TBI control, red lines for TBI and sham IKK2-CA^{GFAP}. Bars indicate Mean±SEM. Statistical comparison by ordinary two-way ANOVA with Tukey's multiple comparisons test. Red lines indicate comparison between GoF sham and TBI, blue lines TBI control and TBI GoF. Exact significances indicated in graphs. Control: pre-TBI (-1d) n = 23; TBI: day 2 n = 16, day 7 n = 11, day 30 n = 10; sham: day 2 n = 4, day 7 n = 4, day 30 n = 3; IKK2-CA^{GFAP}: pre-TBI (-1d) n = 17; TBI: day 2 n = 8, day 7 n = 6, day 30 n = 10; sham: n = 5, day 7 n = 5, day 30 n = 3. Source data are provided as a Source Data file.


a
IKK2
GFAP
IKK2 GFAP
Control
IKK2-CA^GFAP


b
Control
IKK2-CA^GFAP
NG2
GFAP
Overlay
NG2
GFAP
Overlay
Day 1
Day 3
Day 7
Day 15

Supplementary Figure 5: IKK/NF-κB pre-activation in astrocytes disturbs post-traumatic glial scar formation.

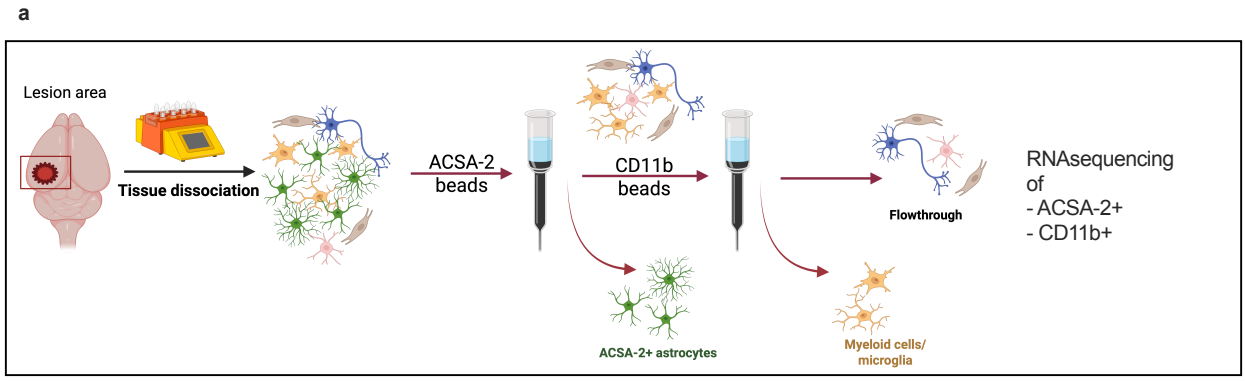
(a) Representative images of GFAP/IKK2 costaining confirms NF-κB driven astrogliosis in IKK2-CA^{GFAP} animals. Scale bar = 50 µm (b) Representative pictures of the scar formation process after TBI. Higher magnification of the scar area, as depicted with the purple squares in Figure 4. The yellow dotted line marks the spread/thickness of the NG2-glia scar, while the distance until NG2-glia reactivity was present as hypertrophic NG2+ cells is indicated with the blue dotted line (day 3, 7, 15). The spread of the GFAP scar is shown with the red dotted line (day 7, 15). Scale bar = 500 µm.

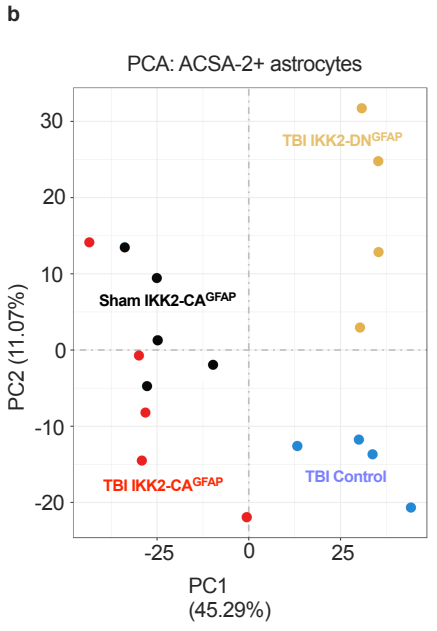


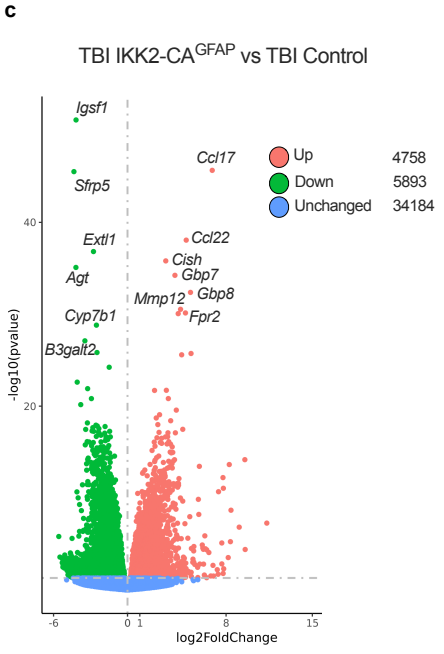
Hein *et al.*, Supplementary Figure 6

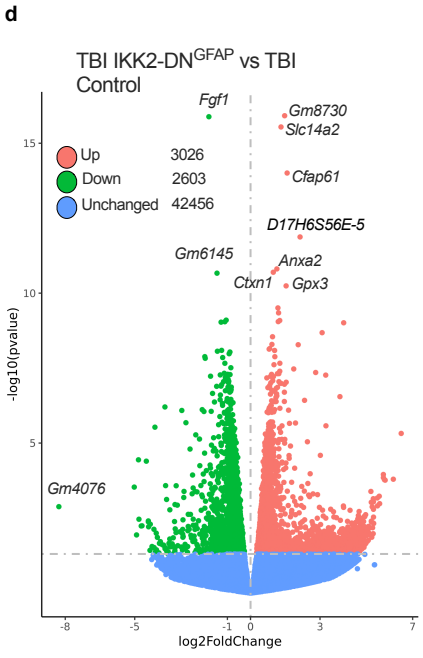
Supplementary Figure 6: Early post-traumatic fibronectin expression is elevated in the lesion area of IKK2-CA^{GFAP} animals.

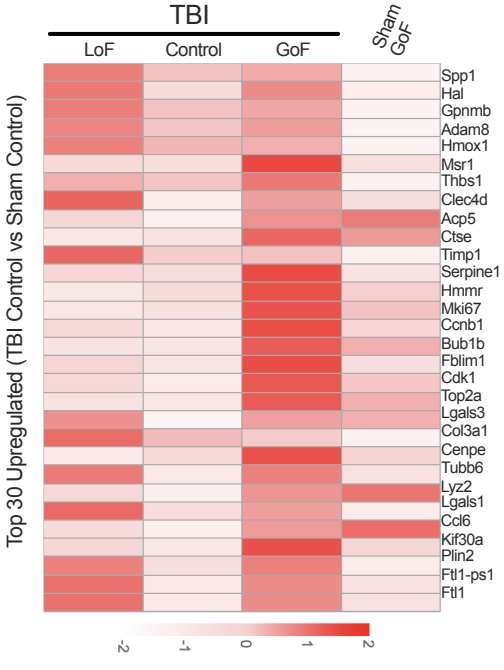
(a) Representative images and (b) quantification of area covered with fibronectin at different time points after TBI in control and IKK2-CA^{GFAP} animals as indicated. Yellow dotted frames indicate areas used for quantification. Scale bars= 500 µm; Bars indicate Mean±SEM. Statistical comparison by ordinary two-way ANOVA with Šidák's multiple comparisons test. n = 3 per group, IKK2-CA day 30: n = 4. (c) Gene expression analyses in bulk insult tissue derived from control (blue) and IKK2-CA^{GFAP} (red) animals after sham-treatment, day 3, 7, 15 and 30 post TBI by qRT-qPCR as indicated. Quantification of *Fn1, Dcn, Chst11, Vcan, Col1a2, Mmp12, Tgfb1* and *Cstb* representing genes related to extracellular matrix (ECM) and scar formation is shown. Control: sham n = 9 (*Mmp12* n = 6), day 3 n = 6 (*Chst11* n = 8), day 7 n = 10 (*Fn1/Mmp12* n = 9, *Chst11* n = 8, *Vcan* n = 11), day 15 n = 8 (*Fn1/Cstb* n = 5, *Col1a2* n = 7, *Mmp12* n = 9), day 30 n = 5; IKK2-CA^{GFAP}: sham n = 5, day 3 n = 7 (*Vcan* n = 6, *Chst11/Col1a2/Tgfb1* n = 8), day 7 n = 5, day 15 n = 3, day 30 n = 4. Graphs indicate Mean±SEM. Statistical comparison by ordinary two-way ANOVA with Tukey's multiple comparisons test. Exact significances indicated in graphs. Source data are provided as a Source Data file.

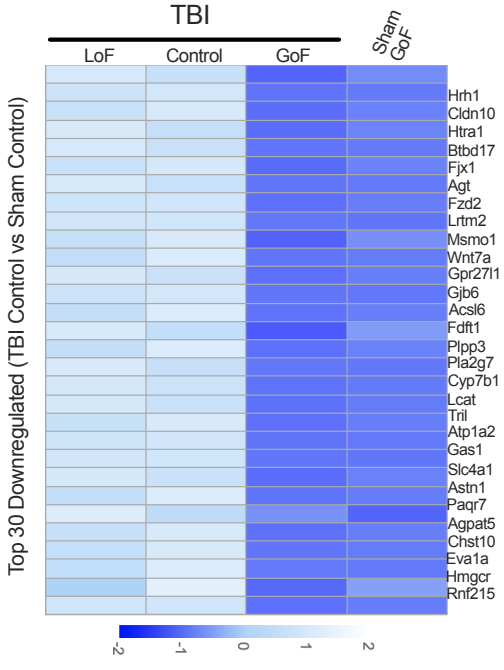








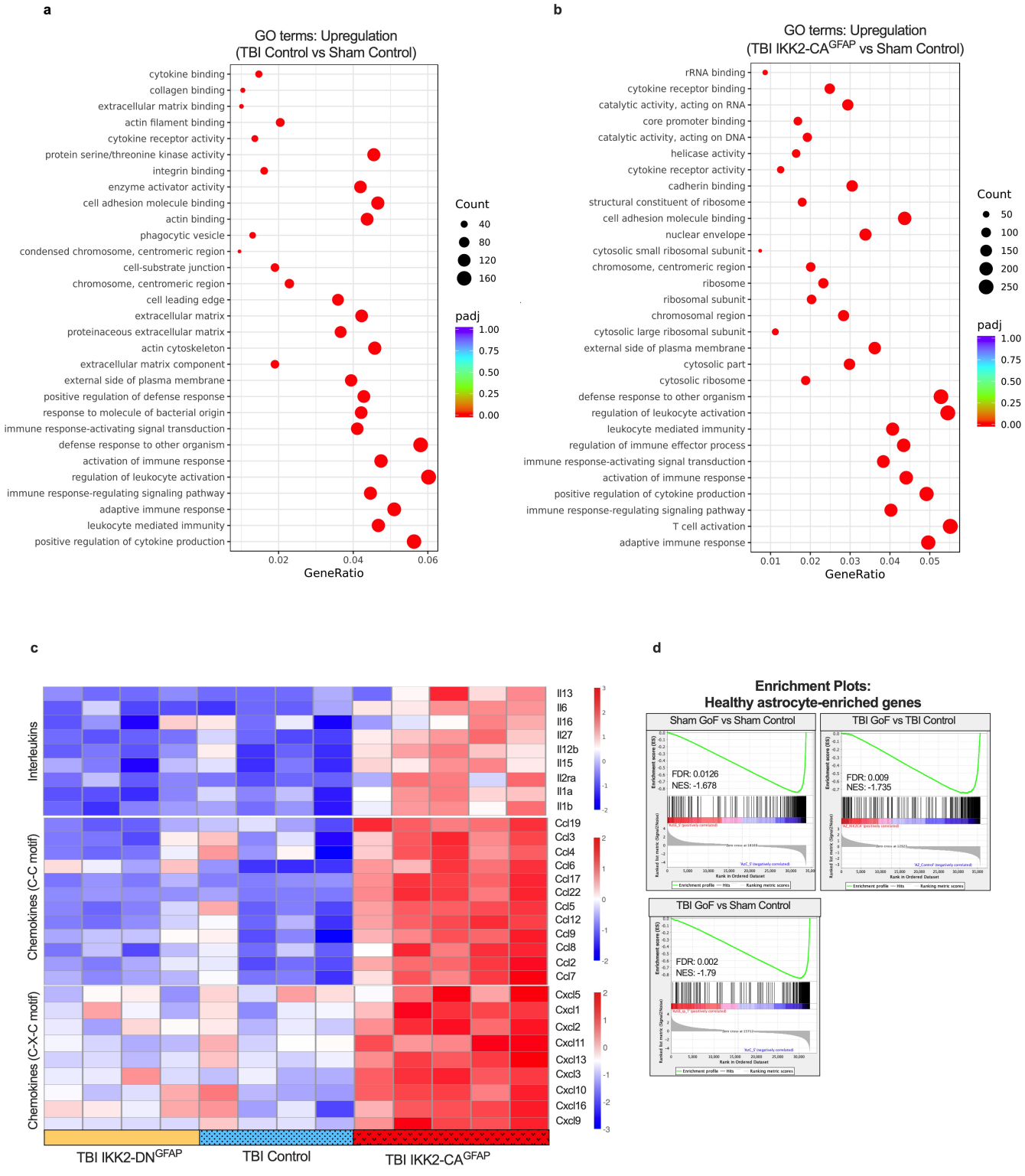




Hein *et al.*, Supplementary Figure 7

Supplementary Figure 7: Astrocytic IKK/NF-κB activation induces aggravated post-traumatic inflammatory responses and affects expression of ECM-associated genes in CD11b+ cells.

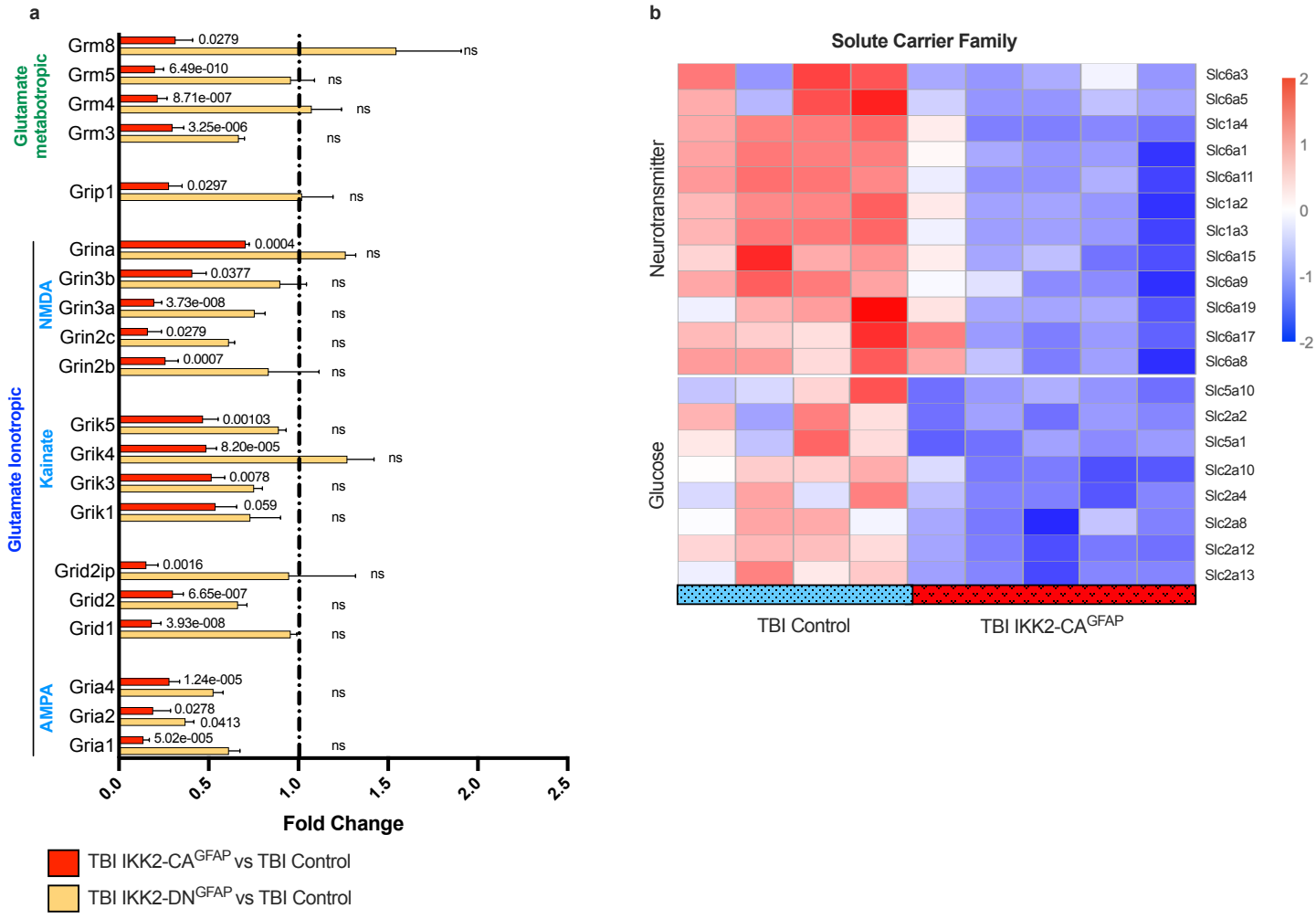
(a) Principal workflow of the MACS purification protocol to isolate ACSA-2+ and CD11b+ cells from brain hemispheres of control, IKK2-CA^{GFAP} (GoF) and IKK2-DN^{GFAP} (LoF) mice at day 3 post TBI used for subsequent RNA sequencing. Image created in BioRender. Hein, T. (2026) https://BioRender.com/k72k301. (b) Principal component analysis shows formation of distinct clusters of post-traumatic control, LoF, GoF as well as sham GoF astrocytes at day 3 post TBI. (c, d) Volcano plots of genes differentially expressed (DEGs) in (c) GoF and (d) LoF astrocytes in comparison to the TBI control astrocytes at day 3 post TBI. (e, f) Heatmap of the top 30 most significantly (padj < 0.05) (e) upregulated and (f) downregulated DEGs (log2FoldChange) after TBI (3 dpi) in control, IKK2-DN^{GFAP} (LoF), IKK2-CA^{GFAP} (GoF) and Sham GoF astrocytes relative to Sham control. Statistics: DESeq2 RNA sequencing analysis (two-sided Wald's test), $|\log_2 \text{FoldChange}| > 0$, p-value < 0.05. FDR correction of p-values (padj) by multiple comparisons test. Source data are provided as a Source Data file.



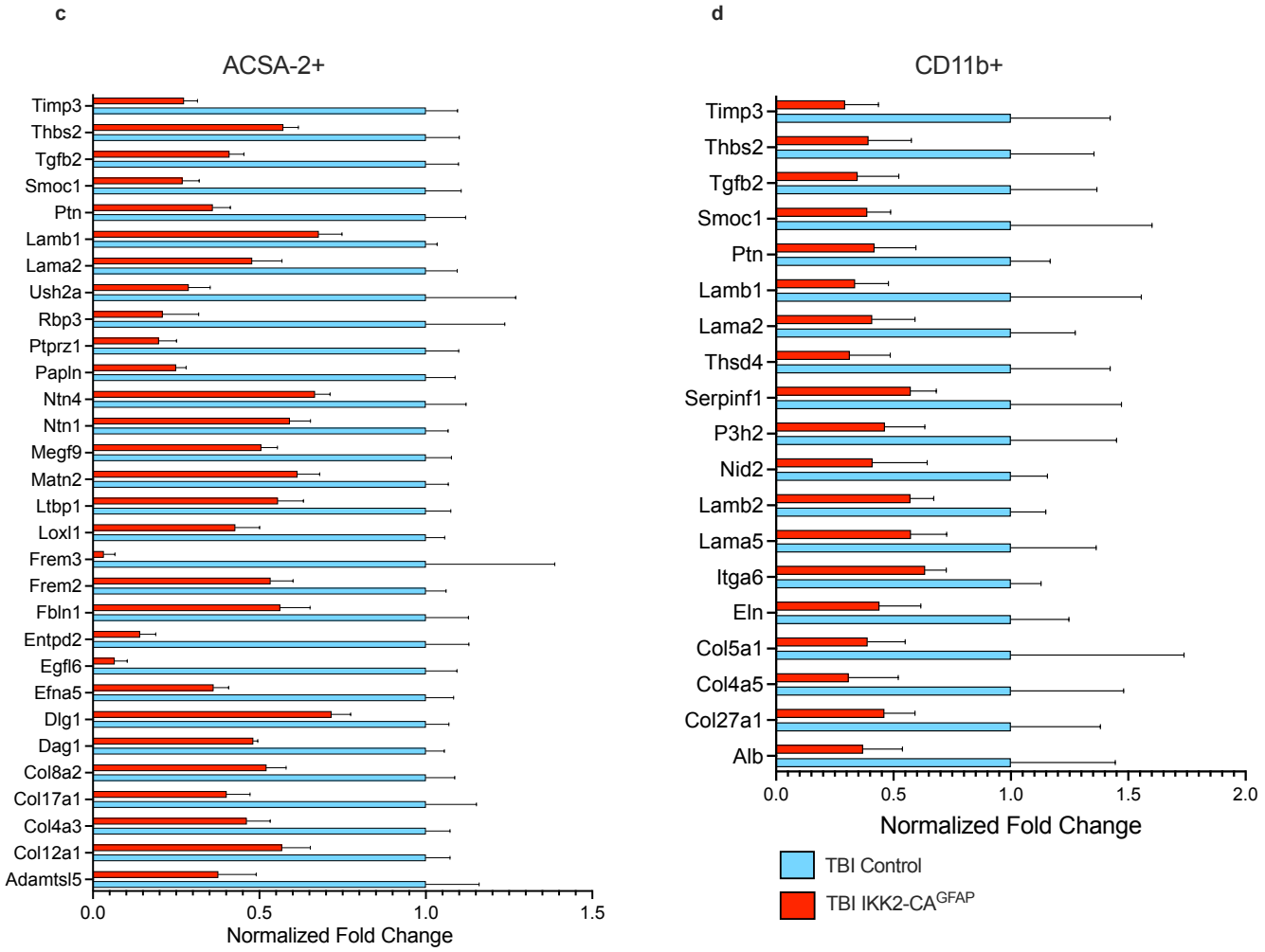
Hein *et al.*, Supplementary Figure 8

Supplementary Figure 8: Astrocytic IKK/NF-κB activation aggravates post-traumatic immune activation and downregulates homeostatic functions in astrocytes.

(a,b) Enrichment charts of the top-upregulated GO terms in (a) TBI control and (b) TBI GoF ACSA-2+ astrocytes as compared to Sham controls at day 3 post TBI. (c) Heatmaps of cytokine and chemokine expression (normalized to log_2) in TBI LoF and TBI GoF astrocytes in comparison to TBI control astrocytes. (d) GSEA plots of ACSA2+ cells analyzed for the expression of 'healthy astrocyte-enriched genes' in Sham GoF and TBI GoF compared to Sham or TBI controls. Statistics: DESeq2 RNA sequencing analysis (two-sided Wald's test), $|log_2FoldChange| > 0$, p-value < 0.05. FDR correction of p-values (padj) by multiple comparisons test. Over- or underrepresentation of gene sets (GSEA analysis) identified by phenotype-based permutation and subsequent multiple hypothesis testing. DOI: 10.1038/ng1180. Source data are provided as a Source Data file.



ECM component (GO:0044420)

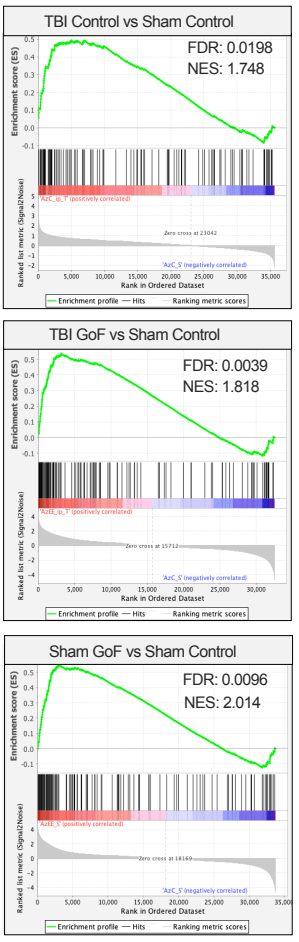


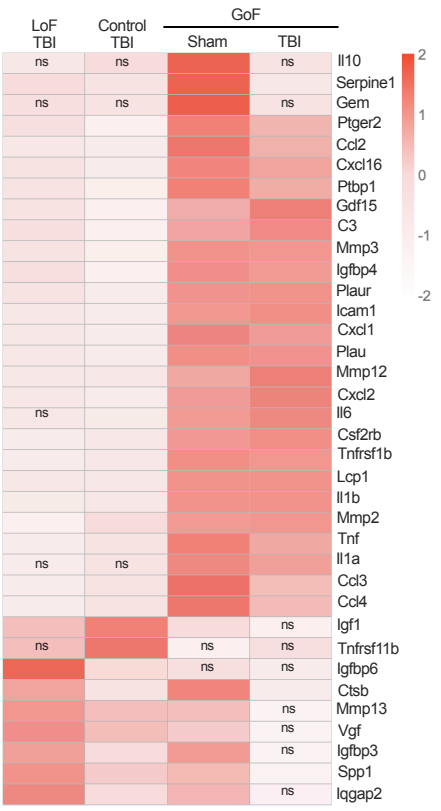
Supplementary Figure 9: Pronounced reduction in neurotransmitter receptor expression and impaired post-traumatic induction of ECM-related genes in IKK2-CA^{GFAP} animals.

(a) Bar chart depicting the post-traumatic downregulation (padj < 0.05) of glutamate receptor genes in TBI LoF and TBI GoF astrocytes compared to TBI Controls. Expression is visualized as Fold Changes relative to TBI controls (mean expression = 1). (b) Heatmap of neurotransmitter and glucose channels significantly downregulated (padj < 0.05) in TBI GoF astrocytes compared to TBI controls (expression presented as log_2). (c, d) Fold change expression of genes included in the GO term 'ECM component' (GO:0044420) in (c) ACSA-2+ (padj = 0.00128) and (d) CD11b+ cells (padj = 6.67E-005) of TBI controls and TBI GoF. Bars indicate Mean±SEM. Statistics: DESeq2 RNA sequencing analysis (two-sided Wald's test), $|log_2FoldChange| > 0$, p-value < 0.05. FDR correction of p-values (padj) by multiple comparisons test. DOI: 10.1038/75556, DOI: 10.1093/genetics/iyad031. Source data are provided as a Source Data file.

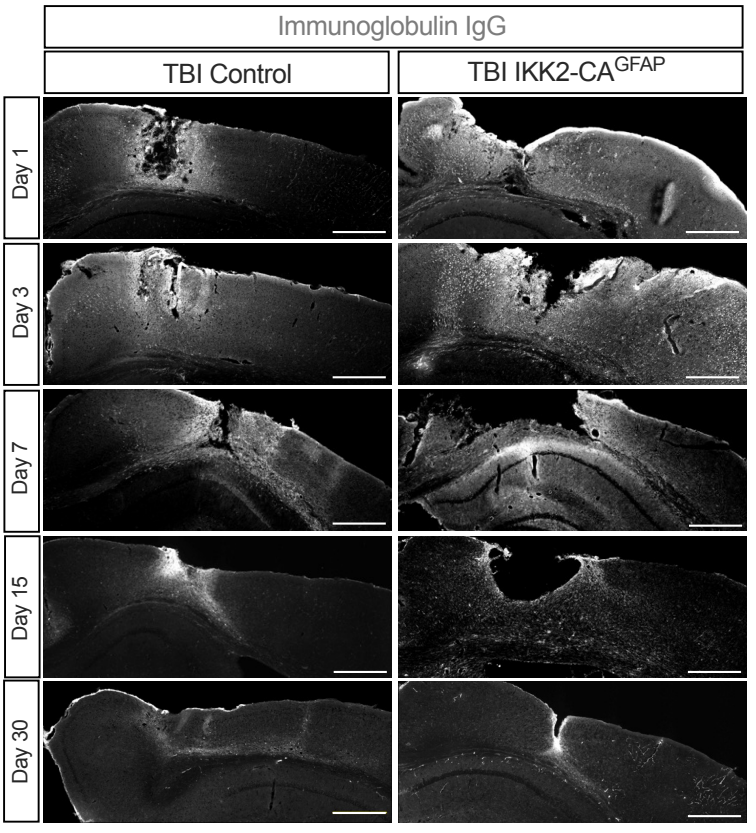
a

Enrichment plots: SASP phenotype (118 genes) in ACSA-2+



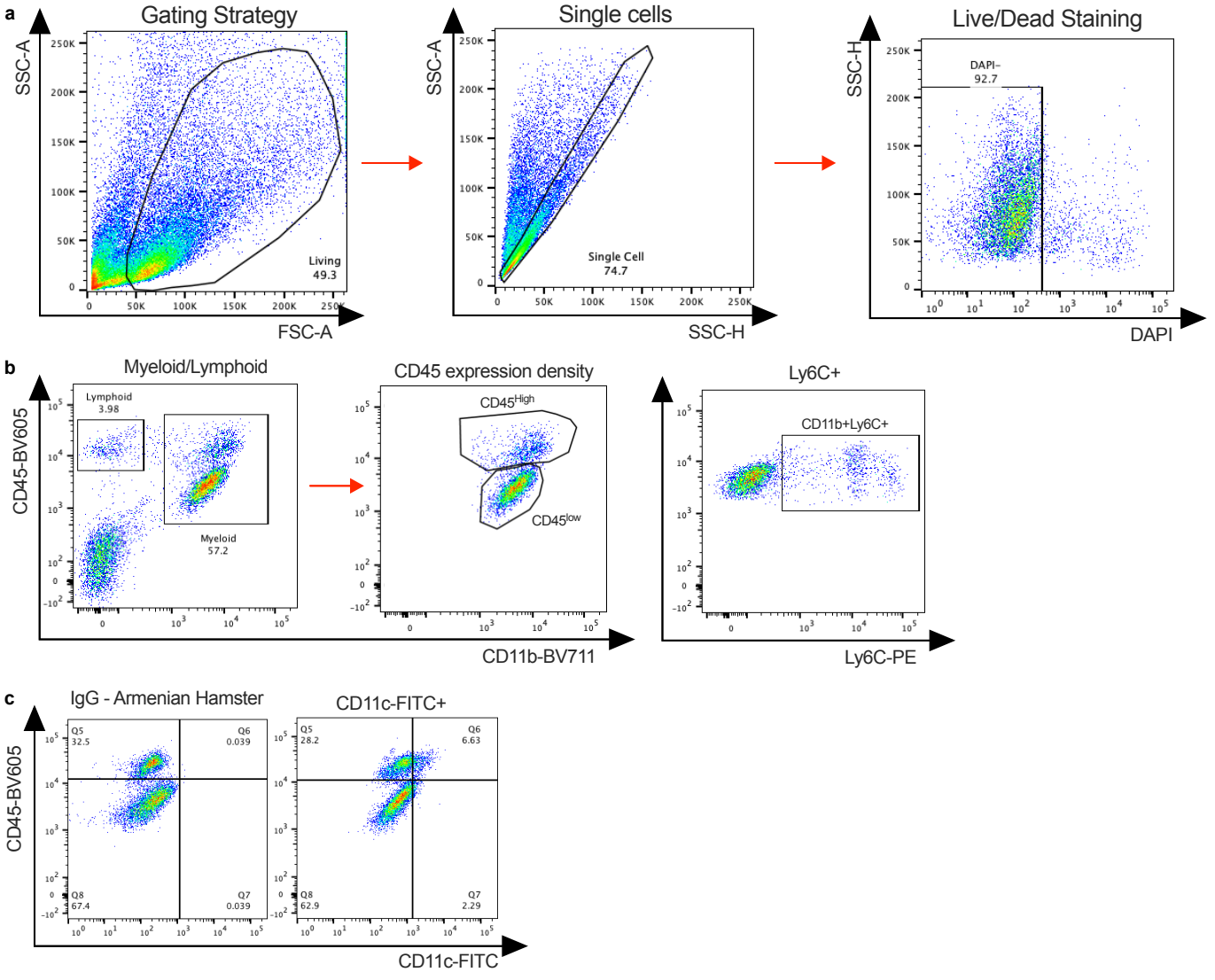


b



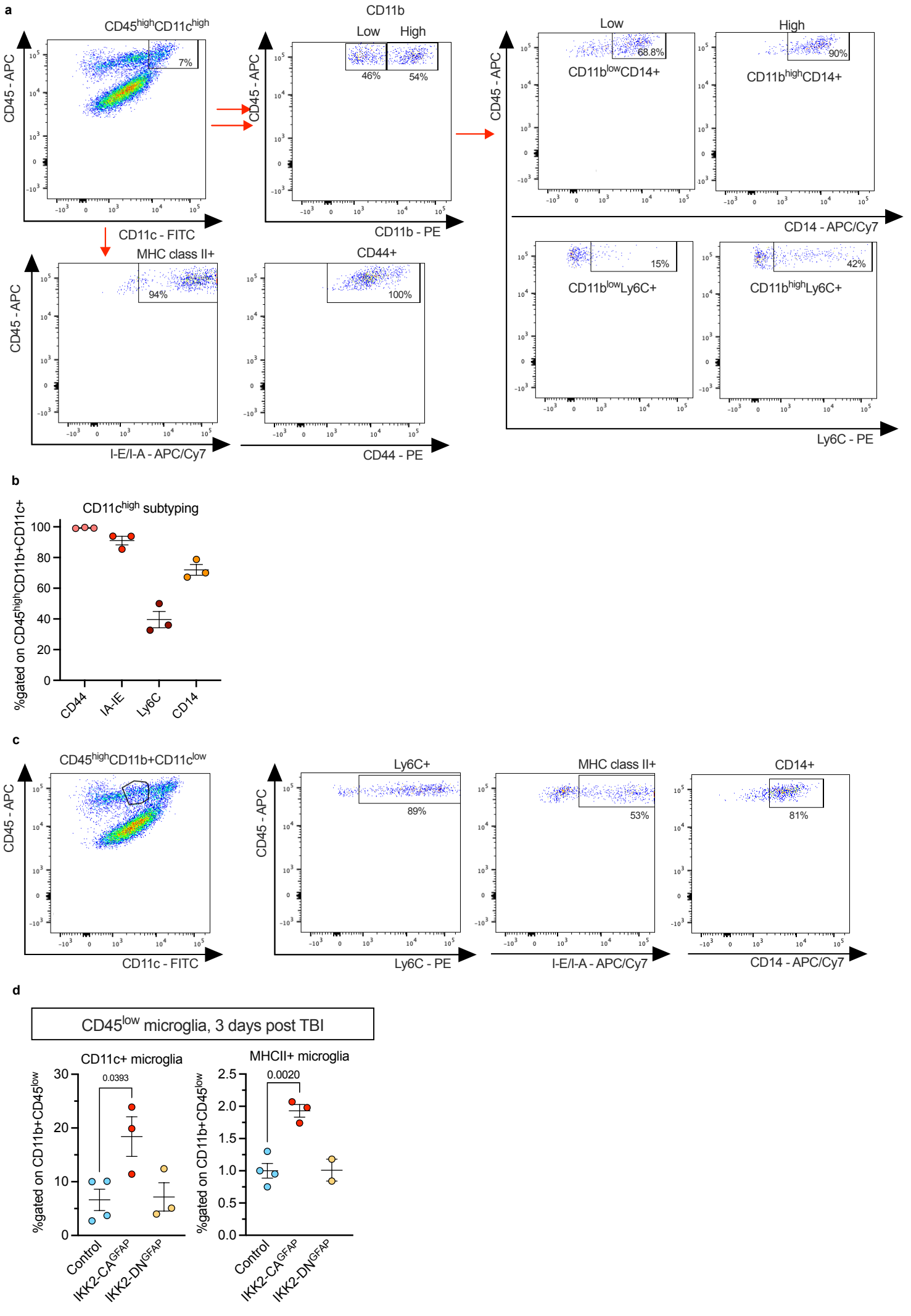
Supplementary Figure 10: Astrocytic IKK/NF-κB activation aggravates TBI-induced SASP development and blood-brain-barrier dysfunction.

(a) GSEA plots and representative heat map of the senescence-associated secretory phenotype (SASP) (SenMayo-Panel, Saul *et al*., 2022) signature in TBI LoF, controls and GoF and Sham GoF in comparison to Sham controls. Gene expression is visualized as $\log_2$ Fold Change. Statistics: DESeq2 RNA sequencing analysis (two-sided Wald's test), $|\log_2 FoldChange| > 0$, p-value < 0.05. FDR correction of p-values (padj) by multiple comparisons test. ns = not significant. GO terms: DOI: 10.1038/75556, DOI: 10.1093/genetics/iyad031. Over- or underrepresentation of gene sets (GSEA analysis) identified by phenotype-based permutation and subsequent multiple hypothesis testing. DOI: 10.1038/ng1180. (b) Immunohistological staining of IgG at different timepoints after TBI in Control and IKK2-CA^{GFAP} animals is shown. In IKK2-CA^{GFAP} animals, a more widespread IgG staining is visible compared to controls from 1-15 dpi indicating enhanced blood-brain-barrier disruption post TBI. Scale bars = 500 µm.


a
Gating Strategy
SSC-A
FSC-A
Living
49.3
Single cells
SSC-A
SSC-H
Single Cell
74.7
Live/Dead Staining
SSC-H
DAPI
DAPI-
92.7
b
Myeloid/Lymphoid
CD45-BV605
CD11b-BV711
Lymphoid
3.98
Myeloid
57.2
CD45 expression density
CD45High
CD45low
Ly6C+
CD11b+Ly6C+
Ly6C-PE
c
IgG - Armenian Hamster
CD11c-FITC+
CD45-BV605
CD11c-FITC
Q5
32.5
Q6
0.039
Q8
67.4
Q7
0.039
Q5
28.2
Q6
6.63
Q8
62.9
Q7
2.29

Supplementary Figure 11: Gating strategy of peripheral infiltrates and resident microglia.

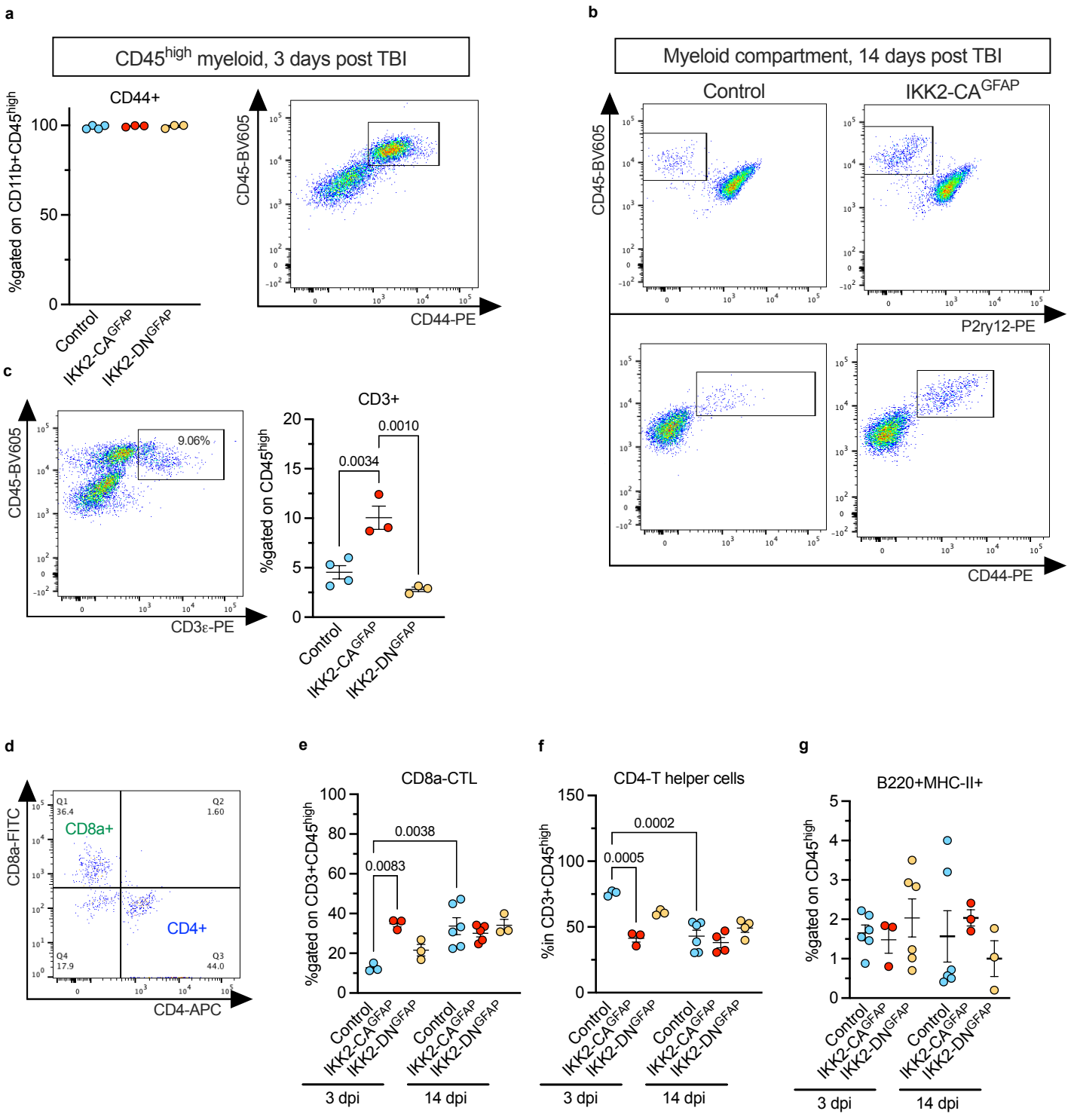
(a) Representative gating strategy for brain-infiltrating leukocyte populations. (b) Representative gating strategy for identification of CD45 and Ly6C expression in myeloid cells. (c) Scatter plot depicting identification of CD11c+ myeloid populations utilizing isotype (Armenian Hamster IgG) controls to exclude false positives.



Hein *et al.*, Supplementary Figure 12

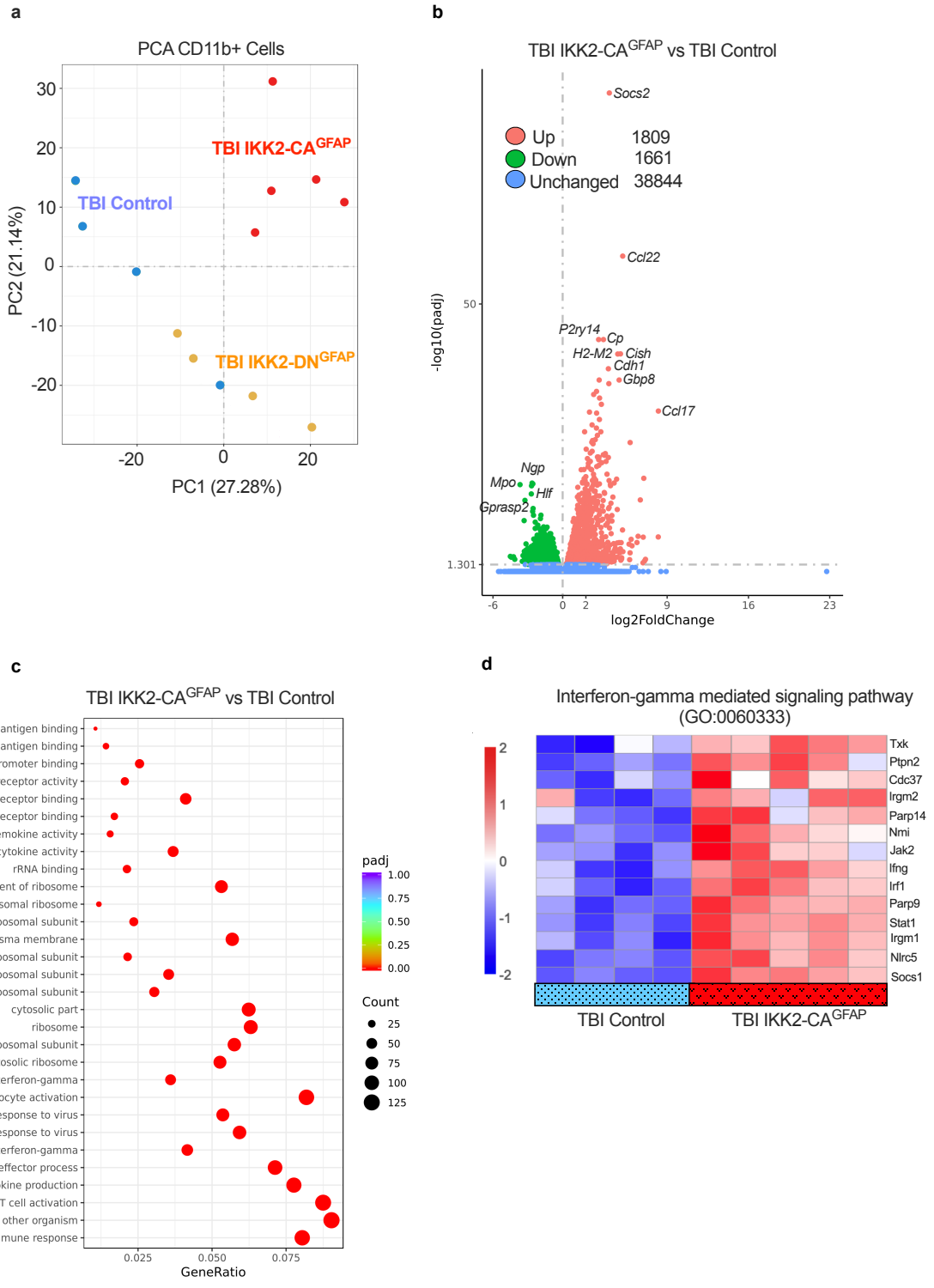
Supplementary Figure 12: Immune phenotyping of myeloid CD11c+ subsets at day 3 post TBI

(a) Representative staining of Ly6C, I-A/I-E (MHC class II) and CD14 in $CD45^{high}CD11b+CD11c^{high}$ population of IKK2-CA^{GFAP} animals at day 3 post TBI. (b) Quantification of CD44, I-A/I-E, Ly6C and CD14 expression in $CD11c^{high}$ subset. (c) Representative staining of Ly6C, I-A/I-E (MHC class II) and CD14 in $CD45^{high}CD11b+CD11c^{low}$ population of IKK2-CA^{GFAP} animals at day 3 post TBI. (d) Quantification of CD 11c and MHC class II expression in $CD45^{low}CD44-$ microglia at day 3 post TBI. Bars indicate Mean±SEM. Statistical comparison by ordinary two-way ANOVA with Tukey's multiple comparisons test. Exact significances indicated in graphs. Source data are provided as a Source Data file.


a
CD45high myeloid, 3 days post TBI
CD44+
%gated on CD11b+CD45high
100
50
0
Control
IKK2-CAGFAP
IKK2-DNGFAP
CD45-BV605
CD44-PE
b
Myeloid compartment, 14 days post TBI
Control
IKK2-CAGFAP
CD45-BV605
P2ry12-PE
CD44-PE
c
CD45-BV605
9.06%
CD3ε-PE
CD3+
%gated on CD45high
0.0034
0.0010
20
15
10
5
0
Control
IKK2-CAGFAP
IKK2-DNGFAP
d
CD8a-FITC
Q1
36.4
Q2
1.60
CD8a+
CD4+
Q4
17.9
Q3
44.0
CD4-APC
e
CD8a-CTL
%gated on CD3+CD45high
0.0038
0.0083
100
80
60
40
20
0
Control
IKK2-CAGFAP
IKK2-DNGFAP
3 dpi
14 dpi
f
CD4-T helper cells
%in CD3+CD45high
0.0002
0.0005
150
100
50
0
Control
IKK2-CAGFAP
IKK2-DNGFAP
3 dpi
14 dpi
g
B220+MHC-II+
%gated on CD45high
5
4
3
2
1
0
Control
IKK2-CAGFAP
IKK2-DNGFAP
3 dpi
14 dpi

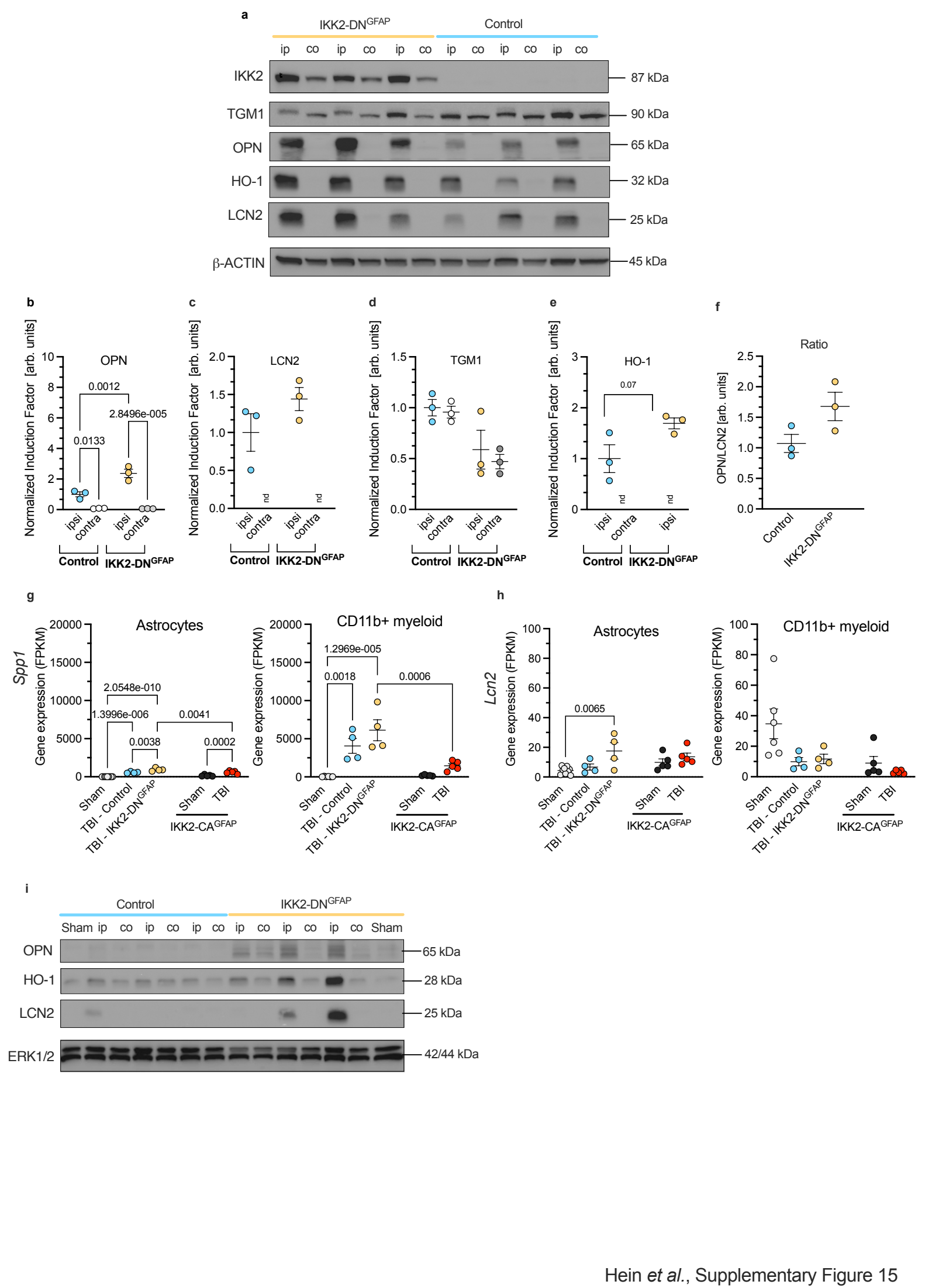
Supplementary Figure 13: IKK/NF-κB activation in astrocytes causes profound alterations in post-traumatic T cell infiltration.

(a,b) To further differentiate between CNS-resident activated microglia and leukocytes invading from the periphery, cells were stained with a combination of CD11b/CD44/CD45 at (a) day 3 post TBI, as well as (b) at day 14 post TBI in addition with the microglial marker P2RY12. (c) Representative scatter dot plot and quantification of CD3+ cells at day 3 post TBI. (d, e, f) Representative scatter dot plot and quantification of CD4 and CD8 subpopulations at day 3 and 14 post TBI. (g) Quantification of B220+MHCII+ lymphoid population at day 3 and 14 post TBI. Bars indicate Mean±SEM. Statistical comparison by ordinary one-way ANOVA with Tukey's multiple comparisons test. Exact significances indicated in graphs. Source data are provided as a Source Data file.


a
PCA CD11b+ Cells
TBI IKK2-CA^GFAP
TBI Control
TBI IKK2-DN^GFAP
PC2 (21.14%)
PC1 (27.28%)
b
TBI IKK2-CA^GFAP vs TBI Control
Up 1809
Down 1661
Unchanged 38844
Socs2
Ccl22
P2ry14
Cp
H2-M2
Cish
Cdh1
Gbp8
Ccl17
Ngp
Mpo
Hlf
Gprasp2
-log10(padj)
log2FoldChange
c
TBI IKK2-CA^GFAP vs TBI Control
peptide antigen binding
antigen binding
core promoter binding
cytokine receptor activity
cytokine receptor binding
chemokine receptor binding
chemokine activity
cytokine activity
rRNA binding
structural constituent of ribosome
polysomal ribosome
small ribosomal subunit
external side of plasma membrane
cytosolic small ribosomal subunit
large ribosomal subunit
cytosolic large ribosomal subunit
cytosolic part
ribosome
ribosomal subunit
cytosolic ribosome
cellular response to interferon-gamma
regulation of leukocyte activation
defense response to virus
response to virus
response to interferon-gamma
regulation of immune effector process
positive regulation of cytokine production
T cell activation
defense response to other organism
adaptive immune response
GeneRatio
padj
Count
d
Interferon-gamma mediated signaling pathway
(GO:0060333)
Txk
Ptpn2
Cdc37
Irgm2
Parp14
Nmi
Jak2
Ifng
Irf1
Parp9
Stat1
Irgm1
Nlrc5
Socs1
TBI Control
TBI IKK2-CA^GFAP

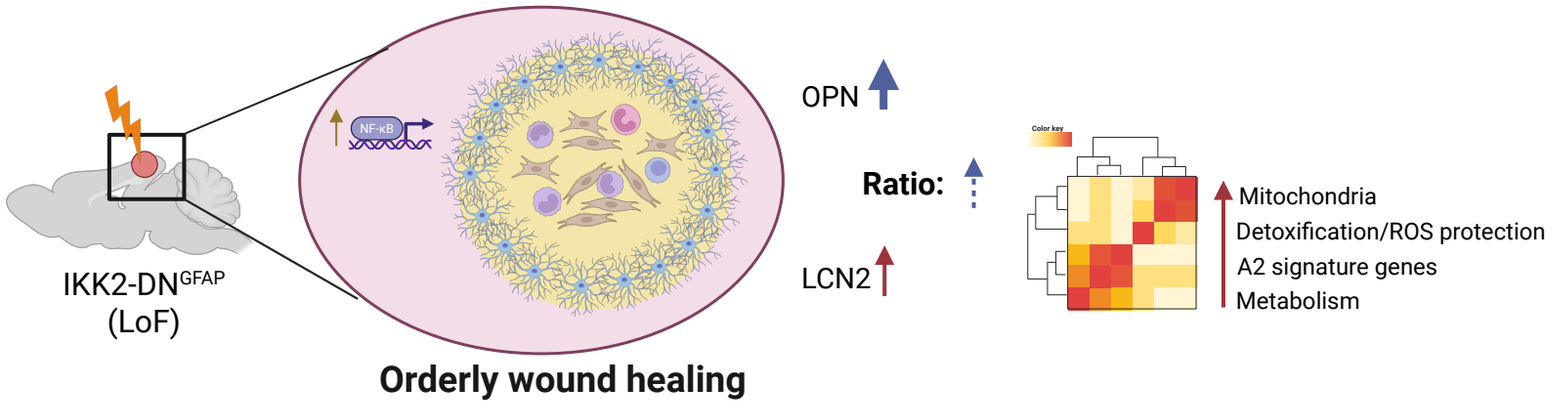
Supplementary Figure 14: CD11b+ myeloid cells of IKK2-CA^{GFAP} animals exhibit an upregulation of interferon-γ associated processes.

CD11b+ cells purified from the TBI insult hemisphere derived of control, IKK2-CA^{GFAP} (GoF) and IKK2-DN^{GFAP} (LoF) mice were used for RNA sequencing at day 3 post TBI. (a) Principal Component Analysis (PCA) showing the distribution of TBI control, TBI GoF and TBI LoF CD11b+ microglia/myeloid cells. (b) Volcano plots of genes differentially expressed (DEGs) in post-traumatic GoF CD11b+ cells when compared to the TBI control cohort. (c) Analysis using the Gene Ontology (GO) database, showing the most significantly upregulated terms of TBI IKK2-CA^{GFAP} CD11b+ cells when compared to the TBI control cohort. Identification by DESeq2, $|\log_2 FoldChange| > 0$, p-value < 0.05. Enrichment; GO terms: DOI: 10.1038/75556, DOI: 10.1093/genetics/iyad031. (d) Heat map ($\log_2$ normalization) of the GO term 'Interferon-gamma mediated signaling pathway' significantly enriched (padj = 2.91e-012) in TBI GoF CD11b+ cells.
Statistics: DESeq2, $|\log_2 FoldChange| > 0$, p-value < 0.05. Enrichment; GO terms: DOI: 10.1038/75556, DOI: 10.1093/genetics/iyad031. Source data are provided as a Source Data file.


a
IKK2-DN^GFAP
Control
ip co ip co ip co ip co ip co ip co
IKK2
TGM1
OPN
HO-1
LCN2
β-ACTIN
87 kDa
90 kDa
65 kDa
32 kDa
25 kDa
45 kDa
b
OPN
Normalized Induction Factor [arb. units]
0.0012
2.8496e-005
0.0133
ipsi contra ipsi contra
Control IKK2-DN^GFAP
c
LCN2
nd
d
TGM1
e
HO-1
0.07
f
Ratio
OPN/LCN2 [arb. units]
Control
IKK2-DN^GFAP
g
Astrocytes
CD11b+ myeloid
Spp1
Gene expression (FPKM)
2.0548e-010
1.3996e-006
0.0041
0.0038
0.0002
1.2969e-005
0.0018
0.0006
Sham
TBI - Control
TBI - IKK2-DN^GFAP
TBI
IKK2-CA^GFAP
h
Lcn2
0.0065
i
Control
IKK2-DN^GFAP
Sham ip co ip co ip co ip co ip co ip co Sham
OPN
HO-1
LCN2
ERK1/2
65 kDa
28 kDa
25 kDa
42/44 kDa

Supplementary Figure 15: Osteopontin expression is increased until day 14 post TBI in the insult tissue of IKK2-DN^{GFAP} animals.

(a) Representative Immunoblot and the corresponding quantifications of (b) TGM1, (c) OPN, (d) HO-1 and (e) LCN2, as well as the (f) OPN/LCN ratio of protein extracts from the ipsilateral insult region (ip) and the contralateral (co) cortical tissue from control (blue) and IKK2-DN^{GFAP} (yellow) animals at day 3 post TBI. Expression was normalized to β-Actin loading control. (g, h) Expression in Fragments per Kilobase Million (FPKM) of (g) *Spp1* and (h) *Lcn2* in ACSA-2+ and CD11b+ cells of control, IKK2-CA^{GFAP} and IKK2-DN^{GFAP} animals at day 3 post TBI as indicated. (i) Immunoblots of control and IKK2-DN^{GFAP} animals showing OPN, HO-1 and LCN2 expression at day 14 post TBI under sham conditions, in the ipsilateral insult region (ip) and contralateral uninjured tissue (co). Bars indicate Mean±SEM. Statistical comparison by ordinary one-way ANOVA with Tukey's multiple comparisons test. Exact significances indicated in graphs; n.d.: not detected. Protein expression presented in arbitrary units (arb. units). Protein data are presented as biological replicates. OPN: Osteopontin (*Spp1*), HO-1: Heme oxygenase 1 (*Hmox1*), LCN2: Lipocalin 2, TGM1: Transglutaminase 1. Source data are provided as a Source Data file.

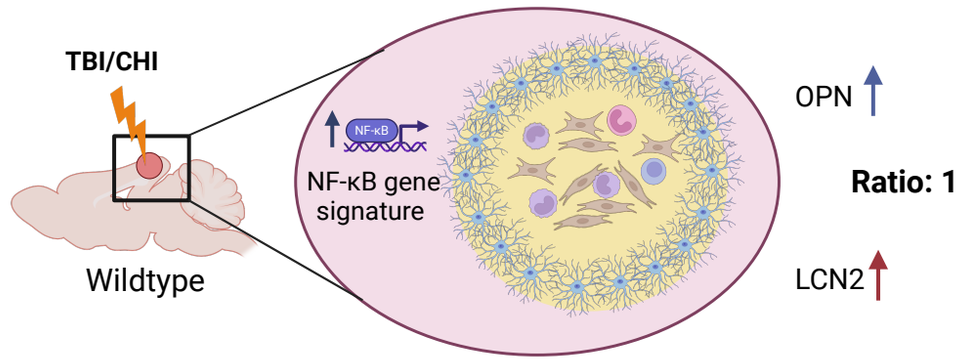


Orderly wound healing

Wound lesion area

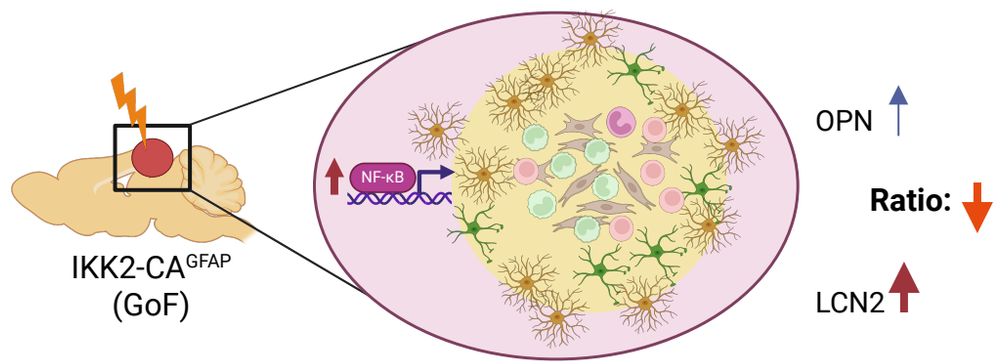
TBI/CHI

Mild behavioral deficits



Orderly wound healing

Pronounced behavioral deficits



Disturbed wound healing

Disorganized scar formation

- dysregulated reactive gliosis
- thin and ill-defined glia scar
- impaired ECM gene regulation
- altered Fibronectin-4 distribution

Altered immune cell regulation

- sustained inflammation and stress
- aggravated cell infiltration
- increased CD11c+MHCII+ DCs
- CD4/CD8 T cell dysbalance

Supplementary Figure 16: NF-κB activation in astrocytes acts as a critical pathological amplification factor promoting detrimental TBI outcome.

Usually, a coordinated, multicellular scar formation process is initiated after TBI in which reactive astrocytes form a defined glial limitans border encapsulating the wound core at the lesion site in order to restrict neurodegenerative processes and promote a beneficial TBI outcome. Our study identifies a strong transient NF-κB gene expression signature in the tissue directly adjacent to the insult area that corresponds well with a dynamic NF-κB activation pattern in astrocytes. To define the NF-κB-regulated processes in this scenario, loss-of-function (IKK2-DN^{GFAP}) and gain-of-function (IKK2-CA^{GFAP}) mouse models for NF-κB modulation in astrocytes were used to monitor TBI pathogenesis. Inhibition of astrocytic NF-κB activation (IKK2-DN^{GFAP}) has selective consequences on the post-traumatic gene expression response including beneficially acting processes such as antioxidant defense, metabolism and mitochondrial functions. These, however, do not affect the overt wound healing process in an obvious manner although osteopontin (OPN), a beneficially acting protein in trauma, was elevated. In contrast, pre-activation of NF-κB in astrocytes (IKK2-CA^{GFAP}) causes global reactive gliosis and an inflammaging-like gene signature possibly phenocopying aged brain conditions which however, trigger an accelerated and aggravated neuroimmune response in response to TBI. Importantly, specific wound healing and scar formation associated processes including epithelial-to-mesenchymal transition (EMT) and astrocyte homeostasis get dampened whereas especially dendritic cells (DCs) arise at the wound lesion area. As a consequence, there is a disorganized glial limitans border and disturbed scar formation associated with transient neurological deficits. In line with this, beneficially acting osteopontin (OPN) expression was significantly reduced while lipocalin-2 (LCN2), a detrimental factor in TBI, was increased in the TBI insult area of IKK2-CA^{GFAP} mice. Figure created in BioRender. Hein, T. (2026) https://BioRender.com/yykywnm

Supplementary Table 1: Top 10 upregulated GO terms found in differently expressed genes three days after TBI in hematoma bulk tissue of wildtype animals ($|\log_2 FoldChange| \geq 1$, padj ≤ 0.05) in (i) biological process, (ii) molecular function and (iii) cellular component. Ranking: ascending P value (color orange). Statistics: Gene ontology enrichment analysis (GO analysis) with PANTHER overrepresentation test (Fisher), FDR corrected and raw P-value < 0.05 (released 24.02.2021). GO Ontology database DOI: 10.5281/zenodo.4495804 (released 2021-02-01).

(i) Biological Process				
GO ID	GO Term	FE	P Value	FDR
GO:0002376	Immune system process	2.61	3.89E-80	6.12E-76
GO:0002682	Regulation of immune system process	2.98	9.47E-66	7.46E-62
GO:0006952	Defense response	3.01	1.37E-64	7.17E-61
GO:0006950	Response to stress	2.14	8.71E-62	3.43E-58
GO:0006954	Inflammatory response	4.85	1.45E-55	4.55E-52
GO:0006907	Response to biotic stimulus	2.79	2.36E-54	6.19E-51
GO:0051707	Response to other organism	2.81	2.87E-54	6.45E-51
GO:0043207	Response to external biotic stimulus	2.81	3.36E-54	6.61E-51
GO:0044419	Interspecies interaction between organisms	2.66	1.22E-52	2.14E-49
GO:0048583	Regulation of response to stimulus	1.91	7.66E-52	1.21E-48
(ii) Molecular Function				
GO:0005515	Protein binding	1.43	7.71E-47	3.58E-43
GO:0005488	Binding	1.22	8.16E-30	1.26E-26
GO:0140375	Immune receptor activity	5.53	1.88E-19	2.19E-16
GO:0019955	Cytokine binding	5.02	2.47E-18	2.30E-15
GO:0005102	Signaling receptor binding	1.75	2.01E-16	1.33E-13
GO:0004896	Cytokine receptor activity	5.72	2.14E-16	1.24E-13
GO:0005201	Extracellular matrix structural constituent	4.26	2.34E-15	1.21E-12
GO:0042802	Identical protein binding	1.64	1.14E-14	5.32E-12
(iii) Cellular Component				
GO:0071944	Cell periphery	1.7	7.87E-57	1.55E-53
GO:0005576	Extracellular region	1.97	3.69E-39	3.63E-36
GO:0110165	Cellular anatomical entity	1.11	1.81E-36	1.19E-33
GO:0005886	Plasma membrane	1.59	5.57E-36	2.74E-33
GO:031012	Extracellular matrix	3.67	2.46E-35	9.67E-33
GO:0030312	External encapsulating structure	3.65	3.52E-35	1.15E-32
GO:0005615	Extracellular space	2.05	2.91E-32	8.16E-30
GO:009986	Cell surface	2.47	2.79E-31	6.86E-29
GO:0062023	Collagen-containing extracellular matrix	3.96	3.76E-31	8.22E-29
GO:0098552	Side of membrane	2.43	1.27E-21	2.50E-19

Supplementary Table 2: Post-traumatic expression of gene included in the KEGG term ko04064 in hematoma bulk tissue of TBI wildtype mice as compared to the wildtype sham cohort. $|\log_2 \text{FoldChange}| \geq 1$, padj ≤ 0.05, Statistical analysis by DESeq2 with alpha-niveau 0.05 (two-sided Wald's test) with n = 7 per group.

KEGG Pathway: NF-kappa B signaling pathway (ko04064)	
Gene Symbol	FC TBI ip vs Sham ip
Btk	8.672
Lrch4	1.595
Ly96	3.416
Relb	1.509
Lbp	3.900
Bcl2a1c	3.813
Lyn	3,843
Nfkb1	1.676
Plcg2	4.681
Trim25	2.91
Syk	4.639
Map3k14	2.095
Plau	3.782
Nfkbia	1.54
Cd40	2.224
Syngr2	3.526
Il1r1	2.881
Irak4	3.964
Il1b	3.393
Ccl4	25.002
Ticam1	1.768
Tnfsf11	4.567
Tnfrsf1a	4.722
Ltbr	3.276
Bcl2a1d	7.192
Traf5	1.633
Nrros	3.464
Icam1	5.258
Traf1	2.815
Pidd1	1.779
Malt1	1.522
Tradd	1.504
Cflar	1.694
Ticam2	6.776
Ltb	2.73
Tlr4	3.934
Tab3	0.615
Birc3	2.564
Myd88	2.376
Ripk1	2.867
Rela	1.635
Tnfsf14	6.516
Ddx58	1.935
Bcl2a1b	22.446
Nfkb2	3.119
Card11	10.038
Blnk	1.735
Tnf	10.638
Cd14	13.63
Bcl2a1a	5.452

Supplementary Table 3: Top 30 upregulated genes out of 1,695 significantly upregulated genes three days post TBI in hematoma bulk tissue of control ($|log_2FoldChange| \geq 1$, padj ≤ 0.05), presented in a descending manner. Genes highlighted in red are regulated by the IKK/NF-κB signaling pathway (Reference: https://www.bu.edu/nf-kb/gene-resources/target-genes/). Statistical analysis by DESeq2 with alpha-niveau 0.05 (two-sided Wald's test) with n = 7 per group. FDR correction of p-values (padj) by multiple comparisons test.

Gene Name	Mean Gene Expression		Fold Change	padj
	Sham	TBI		
Tgm1	1.71	814.05	475.55	6.44E-86
Cd5l	1.53	488.58	319.78	1.62E-44
Spp1	91.11	20620.45	226.34	5.56E-126
Msr1	3.85	713.76	185.55	1.63E-64
Lilr4b	1.30	172.53	132.45	4.01E-39
Hal	2.28	300.85	132.00	3.92E-35
Gpnmb	35.68	4470.13	125.27	1.76E-68
Arg1	2.53	305.82	120.81	5.96E-62
Apoc2	0.98	104.74	107.06	1.52E-34
Cst7	1.38	125.76	91.27	1.48E-35
Lyz2	101.06	8509.46	84.20	4.93E-87
Mmp3	0.72	58.60	81.67	2.15E-22
Timp1	6.18	485.02	78.46	1.07E-61
Mmp13	1.47	114.04	77.46	4.32E-26
Lgals3	12.39	920.70	74.34	8.21E-52
Lrrc15	0.65	45.56	70.44	6.58E-21
Lilrb4a	5.99	375.73	62.69	4.15E-52
Lyz1	10.09	605.10	59.95	3.02E-48
Cyp4f18	1.22	66.64	54.77	3.25E-28
Selp	1.94	104.34	53.89	4.99E-22
Hmox1	103.11	5521.48	53.55	1.41E-258
Ly9	3.72	197.78	53.15	4.39E-59
Clec4d	1.35	71.02	52.53	2.50E-30
Saa3	0.66	34.74	52.24	4.76E-17
Tk1	2.07	99.89	48.19	1.28E-41
Cd300lf	1.73	82.76	47.76	1.25E-30
Mmp10	0.61	28.88	47.06	3.64E-16
Cd22	2.77	129.37	46.66	2.63E-37
Il1rn	1.52	69.42	45.53	8.66E-24
Thbs1	23.71	1066.13	44.96	1.42E-52

Supplementary Table 4: Top 30 downregulated genes out of 90 significantly downregulated genes at day 3 post TBI in control mice ($|\log_2 \text{FoldChange}| \geq 1$, padj ≤ 0.05) presented in a descending manner. Gene highlighted in red is regulated by the IKK/NF-κB signaling pathway (Reference: https://www.bu.edu/nf-kb/gene-resources/target-genes/). Statistical analysis by DESeq2 with alpha-niveau 0.05 (two-sided Wald's test) with n = 7 per group (two-sided Wald's test). FDR correction of p-values (padj) by multiple comparisons test.

Gene Name	Mean Gene Expression		Fold Change	padj
	Sham	TBI		
4930590J08Rik	2.40096136	0.665374087	0.277128195	0.01975208
H60b	51.7750379	14.38267778	0.277791738	8.73E-05
Zfp33b	58.9656352	16.45741114	0.279101736	0.02499712
Lefty2	3.79673977	1.154500427	0.304076786	0.02300876
D830030K20Rik	48.1736112	14.98019774	0.310962732	0.00718903
Olfr464	12.8029819	4.098370545	0.320110626	0.00011904
Cabp4	2.44573544	0.785101417	0.321008317	0.03644781
Kcnh7	830.805294	289.9775378	0.349031885	0.00010015
Adam1b	2.88349092	1.032818175	0.358183259	0.04484757
Gm15319	3.73992321	1.344168395	0.359410694	0.03874707
Baat	3.51633307	1.284010078	0.365155989	0.02661479
Mylk3	32.0063499	11.74313616	0.366900199	9.88E-05
Mab21l2	7.30176838	2.713494119	0.3716215	0.0087419
Htr2a	424.280069	158.5248521	0.373632569	1.83E-15
Dgkh	262.339586	99.77268621	0.380318837	5.85E-08
Clnk	3.33932419	1.281807049	0.383852233	0.04302938
Kcna3	128.55252	49.37924914	0.384117318	7.03E-08
Grin2a	1019.89936	394.3873411	0.386692411	9.45E-05
Gprin3	86.3556531	33.44623547	0.387308002	7.85E-10
Zfp804b	34.3256205	13.3510041	0.388951574	0.00010601
Tenm1	311.527995	122.1994131	0.392258208	0.00014353
Duxbl2	3.21975782	1.263819757	0.39252013	0.04525747
Duxbl3	3.21975782	1.263819757	0.39252013	0.04525747
Pabpc5	21.7941727	8.579199483	0.393646486	4.65E-05
Sv2c	436.218374	173.4890702	0.397711514	7.56E-11
Plcxd3	92.9161284	36.98900436	0.398090245	2.18E-05
Slc9a3	5.87069007	2.343304132	0.399153099	0.01087655
Gm14391	311.122791	124.7629232	0.401008627	8.90E-08
Kcnq3	682.547647	274.2841939	0.401853549	1.52E-10
Dok6	97.4554459	39.41961807	0.404488612	6.30E-05

Supplementary Table 5: Top 10 downregulated GO terms found in differently expressed genes at day 3 after TBI in control mice ($|\log_2 FoldChange| \geq 1$, padj ≤ 0.05) in (i) biological process, (ii) molecular function and (iii) cellular component. Ranking: ascending P value. Statistics: Gene ontology enrichment analysis (GO analysis) with PANTHER overrepresentation test (Fisher), FDR corrected and raw P-value < 0.05 (released 24.02.2021). GO Ontology database DOI:10.5281/zenodo.4495804.

(i) Biological Process				
GO ID	GO Term	FE	P Value	FDR
GO:0071805	Potassium ion transmembrane transport	13.18	1.42E-06	2.23E-02
GO:0099537	Trans-synaptic signaling	7.17	1.61E-06	1.26E-02
GO:0098660	Inorganic ion transmembrane transport	5.97	2.64E-06	1.39E-02
GO:0006813	Potassium ion transport	11.31	3.76E-06	1.48E-02
GO:0099536	Synaptic signaling	6.5	3.80E-06	1.20E-02
GO:0007268	Chemical synaptic transmission	6.79	8.48E-06	2.23E-02
GO:0098916	Anterograde trans-synaptic signaling	6.79	8.48E-06	1.91E-02
GO:0042391	Regulation of membrane potential	5.8	9.95E-06	1.96E-02
GO:0055085	Transmembrane transport	3.95	1.18E-05	2.07E-02
GO:0034220	Ion transmembrane transport	4.26	2.57E-05	4.05E-02
(ii) Molecular Function				
GO:0022836	Gated channel activity	8.1	5.49E-07	2.55E-03
GO:0022843	Voltage-gated cation channel activity	13.28	1.36E-06	3.15E-03
GO:0015079	Potassium ion transmembrane transporter activity	11.82	2.84E-06	4.40E-03
GO:0005216	Ion channel activity	6.28	5.09E-06	5.92E-03
GO:0030594	Neurotransmitter receptor activity	14.28	5.39E-06	5.01E-03
GO:0098960	Postsynaptic neurotransmitter receptor activity	18.97	9.28E-06	7.19E-03
GO:0022832	Voltage-gated channel activity	9.75	9.62E-06	6.39E-03
GO:0005244	Passive-transmembrane transporter activity	9.75	9.62E-06	5.59E-03
GO:0022803	Passive transmembrane transporter activity	5.65	1.24E-05	6.42E-03
GO:0015267	Channel activity	5.65	1.24E-05	5.78E-03
(iii) Cellular Component				
GO:0099699	Integral component of synaptic membrane	11.58	2.23E-08	4.38E-05
GO:0099056	Integral component of presynaptic membrane	18.05	2.41E-08	2.37E-05
GO:0099240	Intrinsic component of synaptic membrane	10.68	4.63E-08	3.03E-05
GO:0098889	Intrinsic component of presynaptic membrane	16.36	4.97E-08	2.44E-05
GO:0045211	Postsynaptic membrane	8.7	7.13E-08	2.80E-05
GO:0099055	Integral component of postsynaptic membrane	12.39	3.79E-07	1.24E-04
GO:0098936	Intrinsic component of postsynaptic membrane	11.76	5.52E-07	1.55E-04
GO:0005887	Integral component of plasma membrane	3.4	1.18E-07	2.90E-04
GO:0042734	Presynaptic membrane	10.58	1.19E-07	2.61E-04
GO:0005886	Plasma membrane	1.99	1.52E-07	2.99E-04

Supplementary Table 6: Top 30 most significantly upregulated genes in astrocytes of IKK2-CA^{GFAP} animals at day 3 post TBI. Genes expression was compared to the corresponding control group after TBI. Statistical analysis by DESeq2 with n = 4 for control, n = 5 for IKK2-CA^{GFAP} animals (two-sided Wald's test). FDR correction of p-values (padj) by multiple comparisons test. Genes highlighted in red are regulated by the IKK/NF-κB signaling pathway (Reference: https://www.bu.edu/nf-kb/gene-resources/target-genes/)

Gene Name	Mean Gene Expression		Fold Change	padj
	Control	IKK2-CA^{GFAP}		
Ccl17	5.72	669.36	117.51	3.01E-42
Ccl22	31.97	874.56	27.19	6.43E-35
Gbp7	505.99	4353.99	8.60	7.81E-33
Cish	44.46	641.13	14.41	2.17E-31
Gbp8	12.31	430.63	34.58	1.39E-29
Mmp12	95.45	1887.78	19.77	8.68E-28
Fpr2	26.92	703.48	26.05	1.97E-27
Siglecg	37.19	645.42	17.31	2.15E-27
H2-M2	12.42	449.89	35.65	3.50E-23
Mcemp1	37.83	799.03	21.04	4.56E-23
Coro2a	216.26	1925.90	8.90	2.66E-19
Rasgrp4	115.18	528.21	4.58	2.66E-19
Jaml	30.15	300.50	9.94	1.89E-18
Kynu	13.82	216.90	15.57	3.13E-17
Gbp4	263.09	1597.95	6.07	9.49E-17
Gbp3	515.12	2593.97	5.03	2.08E-16
Itgae	45.70	519.65	11.35	4.01E-16
Socs2	190.92	1051.23	5.51	9.84E-16
Gpr171	24.85	559.51	22.39	2.62E-15
Gbp5	380.72	2244.72	5.89	4.86E-15
H2-Aa	230.45	3406.87	14.77	5.22E-15
H2-DMa	352.94	3437.33	9.73	5.22E-15
Osm	373.38	3576.88	9.57	1.24E-14
Pim1	433.76	3674.74	8.47	1.24E-14
Nlrc5	267.27	1402.65	5.24	1.49E-14
Cd300lf	358.43	2451.60	6.83	1.69E-14
Cxcl2	122.92	1254.51	10.19	3.66E-14
Gbp9	528.35	2375.69	4.49	3.84E-14
Cd274	253.60	1605.26	6.32	4.16E-14
Tfec	86.01	589.09	6.83	5.02E-14

Supplementary Table 7: Top 30 most significantly upregulated genes in astrocytes of IKK2-DN^{GFAP} animals at day 3 post TBI. Genes expression was compared to the corresponding control group. Statistical analysis by DESeq2 with n = 4 for Control, n = 4 for IKK2-DN^{GFAP} animals (two-sided Wald's test). FDR correction of p-values (padj) by multiple comparisons test.

Gene Name	Mean Gene Expression		Fold Change	padj
	Control	IKK2-DN^{GFAP}		
Gm8730	697.17	1933.79	2.77	1.13E-12
Slc14a2	829.10	2064.22	2.49	1.65E-12
Cfap61	1579.41	4720.83	2.99	4.27E-11
ENSMUSG00000120992	253.08	1113.87	4.40	4.62E-09
Anxa2	3577.72	7871.14	2.20	4.49E-08
Ctxn1	1215.58	2399.93	1.97	4.67E-08
Gpx3	717.45	2080.65	2.90	1.10E-07
1110017D15Rik	938.94	2129.58	2.27	5.38E-07
Serinc2	300.37	694.15	2.31	7.16E-07
Lgals1	2702.62	6476.10	2.40	9.91E-07
AY036118	1083.80	2483.67	2.29	9.91E-07
H2-Eb1	38.52	625.99	16.24	9.91E-07
Rnase2a	6.83	58.14	8.52	2.00E-06
Ly6h	418.97	808.42	1.93	2.59E-06
Dynlt4	572.12	1084.16	1.90	4.33E-06
H2-Aa	225.00	936.90	4.16	4.33E-06
Foxj1	6258.02	11093.63	1.77	5.54E-06
Cd63	9680.76	16897.74	1.75	5.54E-06
Gm19935	2084.69	4280.90	2.05	5.65E-06
Fbln7	1318.47	2729.32	2.07	7.60E-06
Uchl1	595.12	1430.34	2.40	1.11E-05
Cfap126	1229.92	2480.04	2.02	1.20E-05
Rpsa-ps7	112.92	411.48	3.64	1.58E-05
S100a11	724.37	1737.33	2.40	1.83E-05
H2-T23	173.28	1217.10	7.02	1.97E-05
Pcsk2	459.04	1070.80	2.33	2.00E-05
Rpl7a	1429.64	3196.11	2.24	2.00E-05
6820408C15Rik	655.67	1229.69	1.88	2.00E-05
H2-T22	58.63	556.40	9.49	2.00E-05
2410004P03Rik	1758.34	3203.42	1.82	2.10E-05

Supplementary Table 8: Expression of antioxidant/ROS-scavenging genes in ACSA-2+ cells of TBI IKK2-DN^{GFAP} and TBI control animals. Statistical analysis by DESeq2 with n = 4 for Control, n = 4 for IKK2-DN^{GFAP} animals (two-sided Wald's test). FDR correction of p-values (padj) by multiple comparisons test.

Gene Name	Mean Gene Expression		Fold Change	padj
	TBI IKK2-DN^{GFAP}	TBI Control		
Gpx3	1805.078	707.718	2.55	0.00181
Gpx7	461.336	257.874	1.78	0.0058
Gpx8	740.561	498.876	1.48	0.0415
Prdx2	4404.160	2906.789	1.515	0.01172
Prdx5	3803.283	2608.106	1.458	0.0314
Txn1	2503.906	1617.235	1.548	0.0151
Txn2	2273.114	1632.784	1.392	0.0186
Gsta4	1616.497	1084.844	1.490	0.0195
Gstk1	983.613	632.311	1.556	0.0413
Gstm1	12963.831	8890.161	1.458	0.0421
Gstp2	81.686	38.530	2.123	0.0240
Esd	2555.739	1671.047	1.529	0.00648
Mt1	10334.202	6706.456	1.541	0.0464